Bachelor Thesis

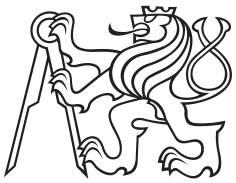

Czech Technical University in Prague

F3

Faculty of Electrical Engineering
Department of Radioelectronics

Image Processing for Digital Holography

Zpracování obrazu pro digitální holografii

Petr Škába

Supervisor: Ing. Karel Fliegel, Ph.D.
May 2021

BACHELOR'S THESIS ASSIGNMENT

I. Personal and study details

Student's name: **Škába Petr** Personal ID number: **474252**

Faculty / Institute: **Faculty of Electrical Engineering**

Department / Institute: **Department of Radioelectronics**

Study program: **Electronics and Communications**

II. Bachelor's thesis details

Bachelor's thesis title in English:

Image Processing for Digital Holography

Bachelor's thesis title in Czech:

Zpracování obrazu pro digitální holografii

Guidelines:

Give an overview of image capture, processing, and reproduction using advanced techniques of digital holography. Focus primarily on image processing concerning speckle noise, its suppression, and methods of assessing the quality of the holographic images. Implement selected methods for digital hologram processing and analysis and verify their performance.

Bibliography / sources:

[1] Schelkens, P., Ebrahimi, T., Gilles, A., Gioia, P., Oh, K.-J., Pereira, F., Perra, C., Pinheiro, A.M.G.: JPEG Pleno: Providing representation interoperability for holographic applications and devices, ETRI Journal, 41 (1), 2019.
[2] Fonseca, E., Fiadeiro, P.T., Bernardo, M.V., Pinheiro, A., Pereira, M.: Assessment of speckle denoising filters for digital holography using subjective and objective evaluation models, Applied Optics, 58 (34), 2019.
[3] Bernardo, M.V., Fernandes, P., Arrifano, A., Antonini, M., Fonseca, E., Fiadeiro, P.T., Pinheiro, A.M.G., Pereira, M.: Holographic representation: Hologram plane vs. object plane, Signal Processing: Image Communication, 68, 2018.

Name and workplace of bachelor's thesis supervisor:

Ing. Karel Fliegel, Ph.D., Department of Radioelectronics, FEE

Name and workplace of second bachelor's thesis supervisor or consultant:

Date of bachelor's thesis assignment: **21.01.2021** Deadline for bachelor thesis submission: **21.05.2021**

Assignment valid until: **30.09.2022**

Ing. Karel Fliegel, Ph.D.	doc. Ing. Josef Dobeš, CSc.	prof. Mgr. Petr Páta, Ph.D.
Supervisor's signature	Head of department's signature	Dean's signature

III. Assignment receipt

The student acknowledges that the bachelor's thesis is an individual work. The student must produce his thesis without the assistance of others, with the exception of provided consultations. Within the bachelor's thesis, the author must state the names of consultants and include a list of references.

.	
Date of assignment receipt	Student's signature

Acknowledgements

I would like to thank my supervisor Ing. Karel Fliegel, Ph.D. of CTU in Prague for understanding, guidance and a lot of patience.

I would also like to extend my thanks to prof. Ing. Aleš Procházka, CSc. of UCT in Prague for valuable insight and helpful advice.

I would also like to thank my family and friends for the unending support.

Declaration

I hereby declare that this submission is my own work and that I have listed all used literature in accordance with the Methodical Instruction on Adherence to Ethical Principles in the Preparation of University Thesis.

In Prague, 15th of May 2021

Abstract

Digital holography is one of the three new promising 3-D imaging methods, which are being considered by the JPEG Committee for a future standardization as JPEG Pleno. Digital holography is already being used in many different fields such as science, engineering, security or entertainment. However, before a wider use of this new imaging method one specific issue needs to be addressed, which is the speckle noise. Several speckle denoising techniques have already been proposed and tested but there are only a few works which address the problem of evaluating the quality of these techniques.

In this work, the reader is first acquainted with the concept of the digital holography which is then followed by a practical experiment in the MATLAB environment to objectively evaluate the denoising quality of several image filters, e.g., Block-matching 3-D filter (BM3D), Frost filter or Wiener filter. The evaluation is based on an entirely new method called Non-Local & Difference Variance Measure (NLDVM), which is proposed in this work. This method does not only evaluate the filtering quality but can also be altered to take the speed of the filtering into the account.

Based on the conducted experiment the best performing filters were found in both the quality and the quality/time ratio categories with the other filters ranked according to their respective performance in the experiment.

Keywords: Digital holography, 3-D, JPEG Pleno, Image processing, Speckle noise, MATLAB, Image filters, BM3D, Frost, Wiener, NLDVM, PSNR, SSIM, MSE

Supervisor: Ing. Karel Fliegel, Ph.D. Praha, Technická 1902/2, 166 27 Praha 6

Abstrakt

Digitální holografie je jednou ze tří nových, slibných 3-D zobrazovacích metod, které výbor JPEG zvažuje pro budoucí standardizaci jako JPEG Pleno. Už nyní se digitální holografie používá v odvětvích jako je věda, inženýrství, bezpečnost nebo zábavní průmysl. Než bude však možné tuto novou zobrazovací metodu plně využít, je třeba vyřešit jeden specifický problém a sice strukturní (speckle) šum. Už bylo navrženo a otestováno několik metod na odstranění tohoto šumu, ale pouze několik prací se zabývalo problémem objektivního hodnocení kvality těchto metod.

V této práci je čtenář nejdříve seznámen s konceptem digitální holografie a poté následuje praktický experiment v prostředí MATLAB, který je zaměřen na objektivní hodnocení kvality filtrace několika obrazových filtrů jako například Block-matching 3-D filtr (BM3D), Frostův filtr anebo Wienerův filtr. Hodnocení je založeno na nově vytvořené metodě zvané Non-Local & Difference Variance Measure (NLDVM), která je v této práci předložena. Tato metoda hodnotí nejen kvalitu filtrace, ale zároveň může být upravena tak, aby brala v potaz také rychlost filtrace.

Na základě provedeného experimentu byly nalezeny nejúčinnější filtry, jak na základě kvality, tak na základě poměru výkonu a času. Ostatní filtry byly seřazeny na základě jejich výkonu v experimentu.

Klíčová slova: Digitální holografie, 3-D, JPEG Pleno, Zpracování obrazu, Strukturní (speckle) šum, MATLAB, Obrazové filtry, BM3D, Frost, Wiener, NLDVM, PSNR, SSIM, MSE

Překlad názvu: Zpracování obrazu pro digitální holografii

Contents

Figures

Tables

Listings

Acronyms

- **1-D** → One-Dimensional space
- **2-D** → Two-Dimensional space
- **3-D** → Three-Dimensional space
- **4K** → 3860×2160 pixels resolution
- **BM3D** → Block Matching and 3-D Filtering
- **CCD** → Charge-Coupled Device
- **CG** → Computer-Generated
- **CMOS** → Complementary Metal-Oxide Semiconductor
- **CPU** → Central Processing Unit
- **dB** → Decibel
- **DCT** → Discrete Cosine Transform
- **DHM** → Digital Holographic Microscopy
- **FIRM** → Fresnel Impulse Response Method
- **FR** → Full-Reference
- **FT** → Fourier Transform
- **GPU** → Graphics Processing Unit
- **HDR** → High Dynamic Range
- **HMD** → Head-Mounted Display
- **JPEG** → Joint Photographic Experts Group
- **JPEG Pleno** → Joint Photographic Experts Group standardization initiative to address the new 3-D imaging methods
- **LCD** → Liquid Crystal Display
- **MATLAB** → Matrix Laboratory
- **MOS** → Mean Opinion Score
- **MSE** → Mean Squared Error
- **NLDVM** → Non-Local & Difference Variance Measure
- **NLDVM$_t$** → Non-Local & Difference Variance Measure per Computational Time
- **NLM** → Non-Local Mean
- **PNG** → Portable Graphics Format
- **PSNR** → Peak Signal-to-Noise Ratio
- **RAM** → Random Access Memory
- **SAR** → Synthetic Aperture Radar
- **SNR** → Signal-to-Noise Ratio
- **SSIM** → Structural Similarity Index Measure
- **VAC** → Vergence-Accommodation Conflict
- **Var** → Variance

Chapter 1

Introduction

For a long time, the innovations in the technological field of imaging have followed a steady curve, mostly given by the Moore's law and the development in the field of electronics. In the recent years, however, there have been a noticeable outburst in the field of imaging techniques, represented by a rapid development of the new technologies. Images and videos in the 4K format, not so long ago thought to be a peak of imaging, are now a common thing with almost every new smartphone, accompanied by the technologies like HDR. Along these new innovations, a new paradigm has arisen, namely a shift from plain 2-D imaging techniques to the 3-D ones. Three representatives of these new 3-D techniques stand out, light fields, point clouds and digital holography. All three are being subject of interest of the JPEG Committee, represented by the new initiative called *JPEG Pleno* [4].

1.1 Motivation

The motivation behind this work is to give the reader an overview of one of these methods, namely the digital holography with a special focus on how to deal with one specific problem that ails it, which is the inherent *speckle noise*, present in every holographic recording, whether its plain old holography or its new digital descendant. Methods of noise suppression will be reviewed in this thesis, along with ways to assess the quality of the said suppression, followed by an implementation of an experiment, to present the reader with the real results, which will be discussed at the end of this thesis.

1.2 Structure

1.2.1 Theoretical part

This work is divided into two main parts. The first, theoretical part will give the reader an overview of the field of the digital holography, focusing mainly on the basics of the digital holography in Chapter 2 , its inherent speckle noise in Chapter 3, methods of the speckle noise suppression in Chapter 4 and the objective evaluation of the suppression quality in Chapter 5.

1.2.2 Practical part

The second part, consisting of Chapter 6 and Chapter 7, is primarily focused on the implementation and an evaluation of an experiment in MATLAB, which is used to demonstrate the theoretical knowledge presented in the previous chapters, while also at the same time, introducing new methods of a quality assessment, which are used to rank the noise suppression methods presented in this experiment.

Details of the experiment

Before every work or experiment, basic ground rules, framework and the aim of the experiment must be established first. Practical experiment in this work is focused specifically on a speckle noise suppression and a quality assessment, but first, it needs to be said, in which part of the process of the digital holography are we operating, from the hologram recording as the first step to the final output as the last step, as seen in Figure 1.1.

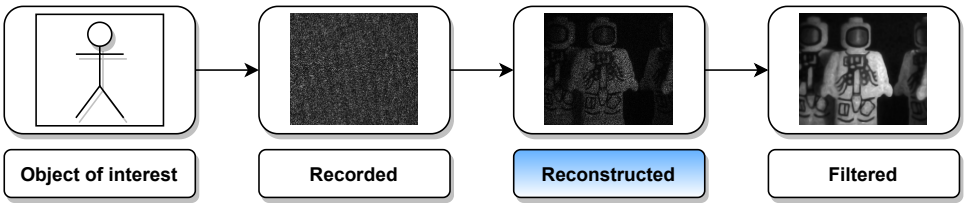

Figure 1.1: Process pipeline of the digital holography, from the recording of the object of interest to the output of the image processing techniques

In this work, as highlighted in Figure 1.1, we will be dealing with the amplitude portion of the numerically reconstructed digital holograms, i.e., in the normal, spatial domain and not in the amplitude/phase domain, i.e., the "raw" hologram domain. This approach is similar to what Elsa Fonseca et al. [5] did in their work. There are several key reasons for this decision. Firstly, digital holography as an imaging method is already being used, even today, but holographic display technology is not. These displays are still commercially rare and expensive so most of the work in the digital holography field is done on the plain old 2-D displays, such as LCD screens. Secondly, when dealing with already reconstructed holograms, we can utilize an already established framework and methods for standard image processing, which is highly beneficial, since the focus of this work is to give the reader an overview of an entirely new imaging technique. Using the already tested and well-known methods can work as a sort of an anchor for the reader, to better understand the topic. And lastly, by using this approach, it is easier to introduce new thoughts into the field, e.g., new methods of speckle noise suppression or quality assessment, since this way we can easily compare new methods to the old, well-known ones. However, unlike the work of Elsa Fonseca et al., this work is focused only on the objective assessment methods, not the subjective ones, as these are beyond the scope of this thesis.

Part I

Theoretical part

Chapter 2

Holography

Basic principle of a holography has been known since 1947 when it was first published by Hungarian-British electrical engineer and physicist Dennis Gabor. Unfortunately, the technology of that time was not advanced enough to perform hologram recording. This changed with the invention of laser in 1960. First holographic recordings were demonstrated almost simultaneously in 1962 by Yuri Denisyuk in the Soviet Union and Emmmet Leith and Juris Upatnieks at the University of Michigan [1]. However, it was not until 1971 that Dennis Gabor was awarded a Nobel Prize in Physics for his invention.

2.1 Recording a hologram

Recording a hologram is very easy in a theory but at the same time it is a great technical challenge to record a hologram of a decent quality. In display applications, visible laser beams are used to provide us with the much-needed wave coherence. Apart from lasers, other components are also needed, like mirrors, beam splitters and expanders.

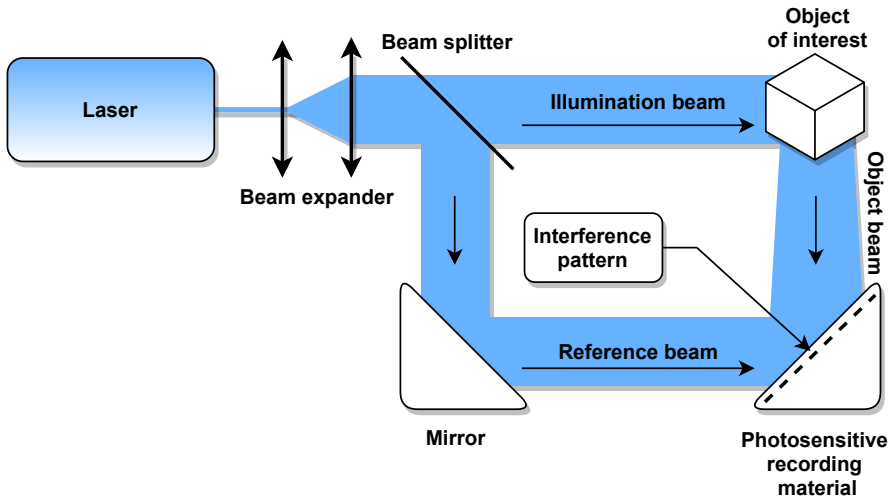

Figure 2.1: Setup for a basic hologram recording, inspired by [1]

To record a hologram, two beams are needed, *reference beam* and *object beam*, as seen in Figure 2.1. In a classical hologram recording, the reference beam does not carry any information about the recorded object, and it is sent directly to the photosensitive recorder. The object beam, on the other hand, is send to the object itself and so it is this beam that carries all the information about the object in the form of a wave amplitude and a phase. Object beam scatters from the object of interest and the scattered light waves then interfere with the waves of the reference beam. These interferences are either destructive or constructive, which creates an intensity fringe pattern recorded on a light-sensitive material, such as photographic plate, as a hologram.

2.2 Reconstructing a hologram

Reconstructing a hologram is once again based on basic physics of waves. Details can be seen in Figure 2.2. In order to reconstruct a hologram, the reference beam is sent to the recorded interference pattern where it gets diffracted, which recreates the original object beam. As noted above, the object beam carries all the information about the object and thus a virtual image of the object is created at the exact same place where the original object was during the initial recording of the hologram.

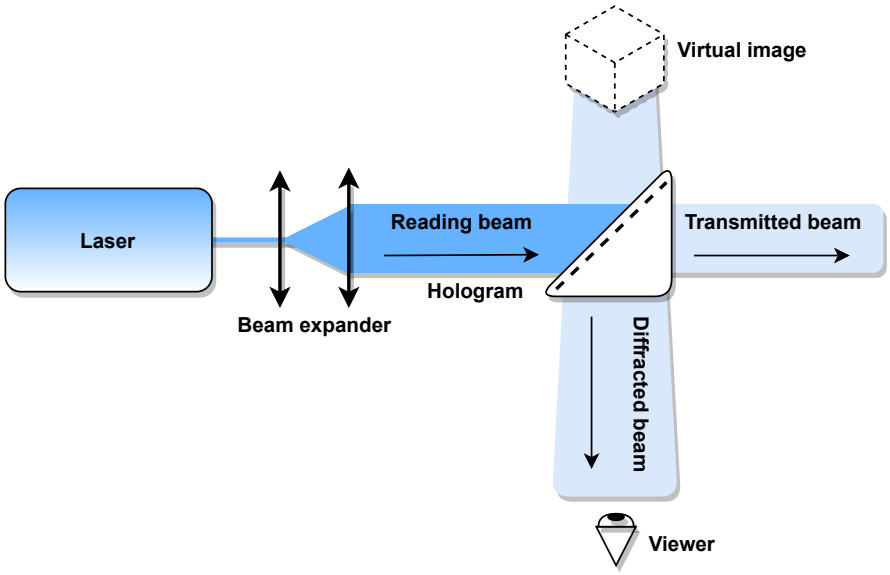

Figure 2.2: Setup for a basic hologram reconstruction, inspired by [1]

This virtual image of the recorded object shows the same behavior as the real object would, e.g., when the viewer moves, the virtual images changes, just a real object would, when observed from different spot. Another example is the recording of several objects at once, like chess pieces. When the viewer moves, the pieces appear to move relative to each other, exhibiting parallax.

2.3 Digital holography

Digital holography is a new approach to holography that is more suitable for modern applications. The basic recording principle is the same as for basic holography but there are a few key differences, as seen in Figure 2.3.

First important difference is present at the hologram recording itself. As the name, digital holography, suggests, this technique works with digital data, which are representing the object and so instead of using a light-sensitive plate, an optical image sensor is used, typically a CCD or a CMOS camera. The image sensor is connected directly to a computer. Reading and visualization of a digital hologram is then done numerically by a computer software.

The 2-D optical image sensor captures the interference pattern as an intensity pattern, which is then sent to the computer for numerical reconstruction. The reconstruction is essential for retrieving the amplitude and phase information from the hologram, which can be later used for additional image processing like creating a 3-D model of the object. This principle is widely used in disciplines like *Digital holographic microscopy* (DHM) to make a highly precise measurements, in *holographic interferometry*, *holographic printing* or in *holographic autostereoscopic displays*.

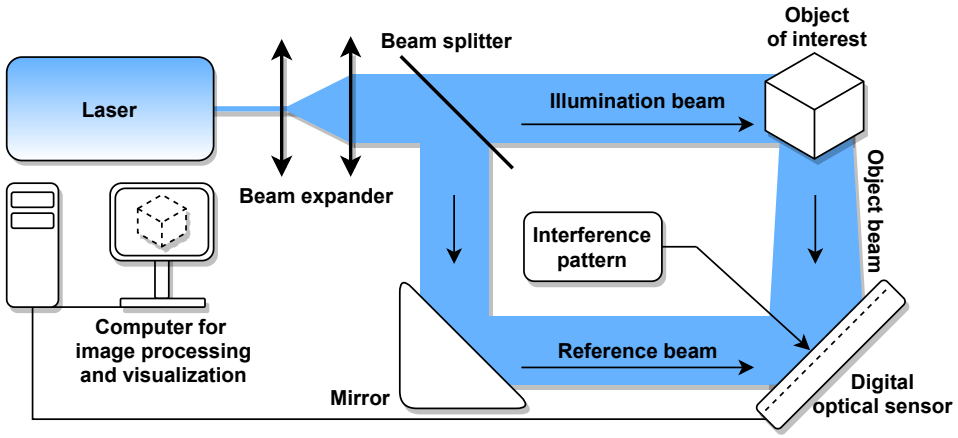

Figure 2.3: Setup for a digital hologram recording, inspired by [1]

Especially the holographic displays are quite interesting. For most people, it is the first thing that comes to mind when talking about holography. Because of the nature of holography, such displays would not only be more interesting for potential users, but also more pleasant to use when compared with displays used today. The users of these displays would suffer less eye fatigue while also avoiding the *vergence-accommodation conflict* (VAC), which plagues other stereoscopic or *head-mounted* (HMDs) displays [4].

Chapter 3

Noise

As with every imaging system, even digital holography is plagued with the ever-present noise. This noise can be divided into two main groups, *technical noise* and *coherent noise*, also known as the, already mentioned, speckle noise. In this chapter, a brief overview of both types of noises will be given to the reader. However, in the rest of this work, only speckle noise and its suppression methods will be discussed and implemented, since the inherent speckle noise is one of the main obstacles in the wider, even commercial usage of the digital holography as an imaging method.

3.1 Technical noise

Aside from common types of noises like electronic noise and quantization noise from analog-to-digital conversion, the main contributor to the technical noise is the *photon noise*, also known as Poisson noise or shot noise.

Individual photon detections can be modeled as independent events that follow the discrete Poisson probability distribution. The number of detected photons N over time interval t can be expressed as

$$Pr(N = k) = \frac{e^{-\lambda t}(\lambda t)^k}{k!}, \tag{3.1}$$

where λ is the expected number of photons per unit time interval. In practice we can model this by Gaussian distribution as the Poisson distribution approaches the Gaussian distribution for large number of photons λ as shown by the Central limit theorem demonstration in Figure 3.1 [6].

3.2 Speckle noise

Speckle noise is one of the main obstacles in recording a high-quality hologram. Speckle noise is classified as a granular, coherent noise and is inherently present in all images which are recorded by a coherent source such as laser. This means the digital holography is heavily affected by this phenomenon. Most real-life objects have a very rough surfaces compared to the scale of the

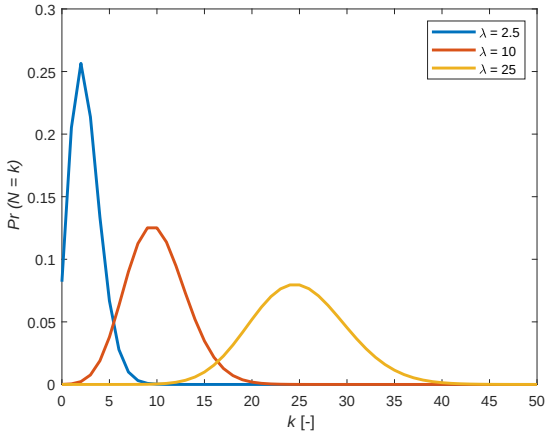

Figure 3.1: Poisson distribution for different λ, demonstration of the Central limit theorem

wavelength of the recording source. In terms of a holography, the object beam can be modeled as a set of individual coherent wavelets. Every individual wavelet hits a slightly different spot on the object of interest and because of the roughness of the object surface, it scatters with a slightly different, random phase. These scattered wavelets interfere with each other either constructively or destructively producing either bright or dark spots depending on the nature of the interference. This behavior creates a very specific pattern as seen in Figure 3.2. This specific speckle noise pattern is also known from other, more common, imaging methods like *Ultrasound* or *Synthetic Aperture Radar* (SAR) [7].

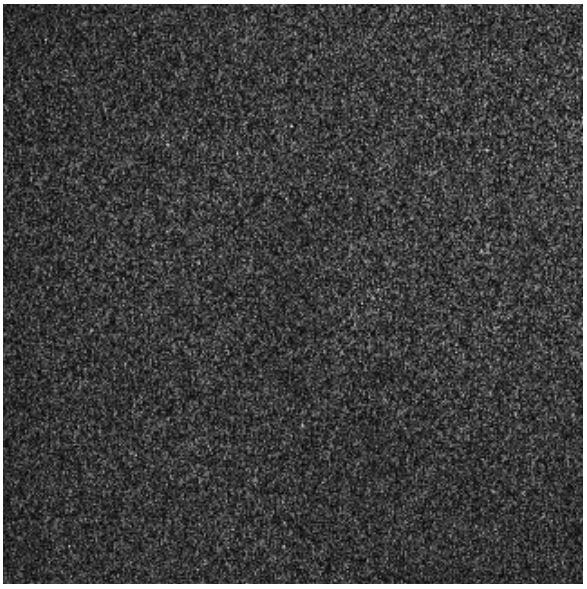

Figure 3.2: Speckle noise in detail on the numerically reconstructed digital hologram "Dice2", which was optically recorded

3.3 Denoising

Speckle noise reduction is crucial to obtain a high-quality hologram and even today, after so many years since first hologram demonstrations, it remains one of the main technical challenges of this imaging technique. Because of the nature of the partly signal-dependent speckle noise, more advanced filtering techniques are needed compared to the filtering of the simple additive noise. There are two main approaches for the speckle noise reduction.

The first approach is labeled as *Optical methods*. This approach is mainly present in the recording stage of the digital holography. Its main concern is the engineering of better coherent light sources, reducing the coherence of the recording light or recording multiple looks of the same object, which are then averaged to produce a final output image. The speckle noise is already naturally suppressed when a hologram is created this way, which makes it easier for the additional image processing.

The second approach is labeled as *Numerical methods*. This approach is mainly present in the reconstruction stage of the digital holography or, as in our case, after the hologram reconstruction. Its main concern is most importantly the spatial filtering, further discussed in the Chapter 4, and Bayesian or non-Bayesian statistical methods [8].

3.4 Speckle noise modeling

Speckle noise is modeled as multiplicative, signal dependent noise also known as *Rayleigh noise*. Let us assume the $I(i, j)$ is the noised, degraded image pixel, then

$$I(i, j) = S(i, j) \cdot N(i, j), \tag{3.2}$$

where $S(i, j)$ is the noise-free pixel and $N(i, j)$ is the normally distributed random noise with unit mean and standard deviation [9].

MATLAB implementation

The speckle noise can be easily modeled in the programming environment MATLAB using standard, non-holographic images. MATLAB already has an in-built function `imnoise()`, which can be used to simulate many different types of image noises. This function is very useful, but for a better understanding of the speckle noise, it is better to implement a Rayleigh noise model, which is then very helpful in subsequent noise filtering and additional image processing. A quick example of how to implement the speckle noise model in MATLAB can be observed in Listing 3.1. It is also worth mentioning, that the `imnoise()` function uses the uniformly distributed noise, as opposed to Eq. (3.2), which uses the normally distributed noise and so the output of each of these implementations will be different for the same initial conditions.

Listing 3.1: The implementation of the speckle noise in MATLAB

```
n = (sqrt(speckle_var) * randn(size(original_image)));
% randn() returns normally distributed random numbers
n = n + speckle_mean;

% I = S + n * S = S * (1 + n) = S * N
noised_image = original_image + original_image .* n;
```

The `orignal_image` is the uint8 grayscale noise-free image and `n` is a normally distributed random value with a variation `speckle_var` and a mean `speckle_mean`.

Effects of this implementation can be observed in Figure 3.3. The image used of this demonstration is Hologram Earth by Kevin Gill under *CC BY 2.0*, modified [10], with the size of 1152×1152 pixels. This picture was converted to grayscale `double` matrix and noised by MATLAB `imnoise()` function with speckle noise with the noise variance $\sigma^2 = 0.5$.

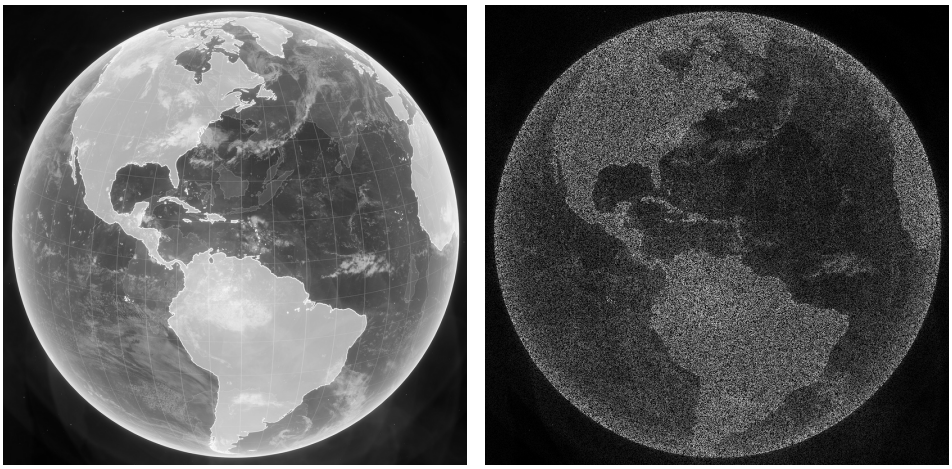

3.3.1 Original grayscale 2-D image

3.3.2 Image with artificially added speckle noise

Figure 3.3: Effect of the speckle noise on a grayscale 2-D image

Chapter 4

Image filtering techniques

This chapter focuses on the image filtering techniques used in the digital holography to suppress the speckle noise. The basis for this work, and the experiment implementation, are the seven filters, belonging to different categories of the image filters, as seen in Figure 4.1, where the used filters are highlighted. These filters were chosen based on their known performance in the field of digital holography, as demonstrated in the works of Elsa Fonseca et al. [5] or Vittorio Bianco et al. [8]. The working principle of each filter is then further explained, after which they are implemented in the practical experiment in the following chapters.

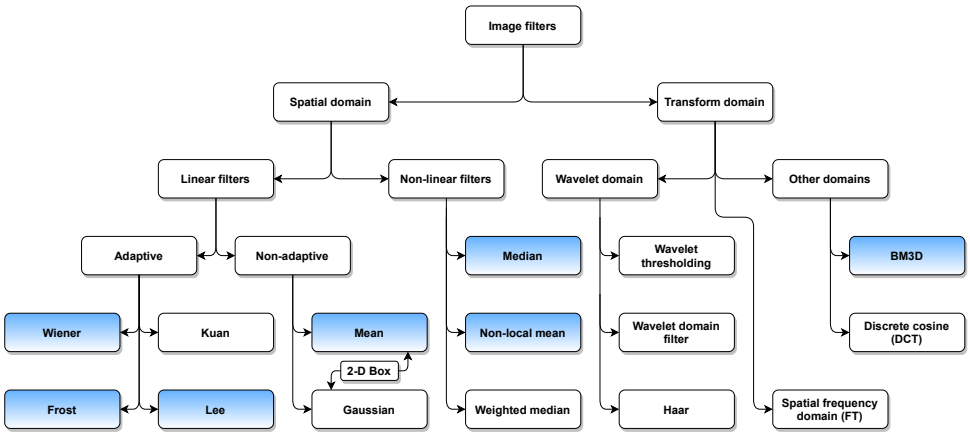

Figure 4.1: Basic classification of the image filtering techniques, inspired by [2]

4.1 BM3D filter

Block matching and 3-D filtering is a novel image denoising filter proposed by Ymir Mäkinen et al. [3] of Tampere University of Technology, Finland, which is considered one of the state-of-the-art strategies for speckle noise suppression in the field of digital holography. This filter falls into the special category known as *collaborative filters* meaning it utilizes both the non-local denoising and transform-based denoising algorithms. See Figure 4.2 which depicts the first and most important stage of the BM3D filtering which is block matching itself, followed by hard thresholding.

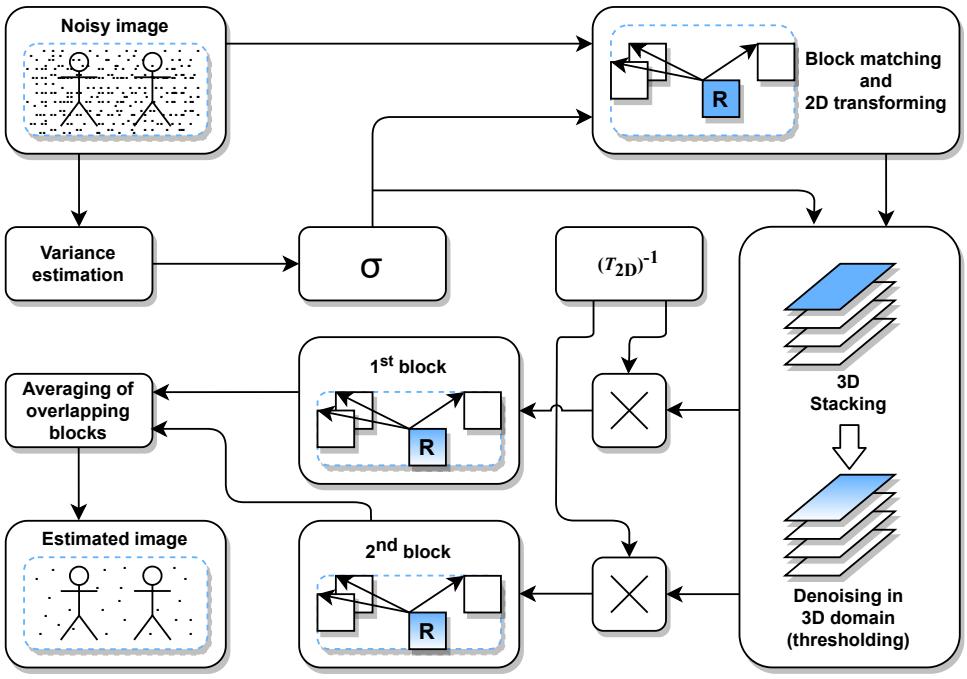

Figure 4.2: First stage of BM3D filtering: the block-matching followed by hard-thresholding, inspired by [3]

At first, we need to identify similar 2-D fragments or blocks within the image and group them together into 3-D arrays called *groups*. This is done by choosing a reference blocks and comparing other blocks with these reference blocks. It is not unusual that the blocks and thus groups overlap with each other. A 2-D transform is then applied, DFT in this case. Another transform, 1-D this time, is then applied on the 2-D spectrum to create a 3-D group. It is in this 3-D domain where shrinkage is performed. Data in groups are subjected to a threshold obtained from original image variance estimation. If a number in a 3-D group falls below this threshold, it is reduced to 0, otherwise the number is preserved.

Groups are then destacked, inverse 2-D transform is applied, and blocks are returned to the original position. By doing this we get a very good estimation of the denoised picture. Because blocks might have been overlapping with one another, we can get many estimations for a single pixel. This is resolved by a simple weighted average of the numbers. This is the first but the most important step in a BM3D filtering. This stage can be then followed by a Wiener filtering to achieve the best results.

4.2 Wiener filter

Linear *Wiener filter*, belonging to the group of *adaptive filters* is arguably one of the oldest and yet still widely used filters to this day. It was first published by an American mathematician Norbert Wiener in 1942, during

his time at Massachusetts Institute of Technology, as a classified document due to its connections to improve radar communications in a war effort. This filter is based on a statistical information retrieved from the image. First, we retrieve the local mean μ and variance σ^2 around each pixel $x(n_1, n_2)$ in a M×N neighborhood as

$$\mu = \frac{1}{NM} \sum_{n_1,n_2 \in \eta} x(n_1, n_2), \tag{4.1}$$

$$\sigma^2 = \frac{1}{NM} \sum_{n_1,n_2 \in \eta} x^2(n_1, n_2) - \mu^2, \tag{4.2}$$

where η represents the M×N neighborhood. These are then used to create an estimate of a noiseless image as

$$y(n_1, n_2) = \mu + \frac{\sigma^2 - \nu^2}{\sigma^2}(x(n_1, n_2) - \mu), \tag{4.3}$$

where $y(n_1, n_2)$ is the estimated output pixel and ν^2 is the noise variance. If ν^2 is not given, MATLAB function `wiener2()` uses the average of all the local variances σ^2 [11].

In MATLAB we can also find the native `deconvwnr()` function as an implementation of the Wiener filter. However, this implementation is non-adaptive and thus less suitable for the use in the digital holography.

4.3 2-D Box filter

Concept of a *Box filter* is an easy one, its most common implementation is also known as *Box blur*. It is a type of convolution filter meaning that we perform a convolution of the image matrix and a smaller window matrix named *kernel* to produce third matrix which is the final, estimated image.

Let us say we center a 3×3 kernel around pixel $\boldsymbol{p}$. This kernel matrix consists only of numbers 1, multiplied by the scalar number $\frac{1}{3^2}$. Convolution of this kernel and the corresponding 9 image pixels around the pixel $\boldsymbol{p}$ produces a local mean of these image pixels which is then used as a new value of the pixel $\boldsymbol{p}$. After that, the kernel moves to another pixel and so on.

This is the most common use of the box filtering. This filter can be further tweaked by changing the values in the kernel matrix to produce different results, e.g., edge detection, sharpening, Gaussian blurring, Frost filtering and more.

4.4 Frost filter

Frost filter, as proposed by Victor S. Frost et al. [12], also belongs to the family of adaptive filters based on the principle of convolution. It was primarily designed to suppress multiplicative noise, which makes it an excellent candidate for speckle noise filtering. It uses the local statistics in a sliding window and an exponential weight to estimate the denoised image. It also does a good job at preserving the edges while suppressing the noise.

Let us say we pick a window $\mathbf{X} = \begin{pmatrix} x_{11} & x_{12} & x_{13} \\ x_{21} & x_{22} & x_{23} \\ x_{31} & x_{32} & x_{33} \end{pmatrix}$ of size 3×3 pixels from the noised image and we wish to denoise the middle pixel. Then we calculate local mean and standard deviation which are later used in an exponential weighting as

$$\alpha = D \cdot \frac{\sigma^2}{\mu^2}, \tag{4.4}$$

where σ^2 is the local variance and μ is the local mean. D is the dampening factor, which can be set be the user to achieve different results. After that we create a distance matrix $\mathbf{R}$ which tells us the distance of other pixels in the window to the middle pixel. Using both the α and $\mathbf{R}$ we calculate the matrix

$$\mathbf{W}_{ij} = e^{-\alpha \cdot \mathbf{R}_{ij}} \tag{4.5}$$

which represents the exponential weight of every pixel in the window. The final estimation of a denoised pixel is then calculated as

$$y(n_1, n_2) = \frac{\mathbf{X} * \mathbf{W}}{\sum \mathbf{W}}. \tag{4.6}$$

From the Eq. (4.6) is clear that the filtration itself is a simple Box filtering as described above. It is not unusual for the image filters to use the concept of Box filtering. The main idea behind the Frost filter is to find the convolution kernel $\mathbf{W}$ itself.

4.5 Lee filter

Lee filter, as proposed by Jong-Sen Lee [13] in 1980, is yet another adaptive filter using the local statistics in a sliding window to estimate a noiseless image. Lee filter is also quite lightweight when compared with the other filters which suppress multiplicative noise as it requires no transformations or complicated matrix calculations while at the same time it offers very good results in noise suppression and edge preservation.

Once again it begins with a construction of the moving window or kernel in which we make use of the local statistics to estimate the denoised pixel value as

$$y(n_1, n_2) = \mu_k + W[x(n_1, n_2) - \mu_k], \tag{4.7}$$

where μ_k is the mean of the pixels in the window, W is the weight function and $x(n_1, n_2)$ is the central, noised pixel which we are trying to replace with our new estimation. W is obtained as

$$W = \frac{{\sigma_k}^2}{{\sigma_k}^2 + \sigma^2}, \tag{4.8}$$

where ${\sigma_k}^2$ is the variance of the pixels in the window and σ^2 is the variance of the entire image. It is clear, that this filter is truly lightweight when compared with the BM3D or Frost filter mentioned above while at the same time the results and especially quality/time ratio of these filters are comparable.

4.6 Median filter

Median filter uses a rather straightforward approach to the filtering. This filter takes the selected input pixel and replaces its value with the median of a surrounding neighborhood. If no specific neighborhood is selected, the MATLAB function `medfilt2()` uses the 3×3 neighborhood, which is also used in this work. Median filter is usually used when dealing with "salt and pepper" noise but in the case of digital holography and speckle noise, it can also find its value. Median filter, which can be considered lightweight, can be easily combined with other forms of more complicated filtering to produce even better results.

4.7 Non-Local Mean filter

The principle of a local mean filter is quite simple, it replaces the pixel value with the mean of the surrounding pixels in a defined neighborhood as explained above in the section about Box filter. The variance law in probability theory tells us that if we average nine pixels of the same color, the noise standard deviation will be reduced to one third of its value. But there is no guarantee that the pixels of the same color will be found in the neighborhood of the targeted pixel and that is where *Non-Local Mean filter* (NLM), proposed by Antoni Baudes et al. [14], comes into play. This filter uses two different neighborhoods called windows, bigger search window and smaller comparison window.

Let us say we want to find a denoised value of a random pixel $\boldsymbol{p}$. In the bigger search window, we select another pixel $\boldsymbol{q}$ and we form smaller comparison windows around both pixels. The we calculate weighted Euclidean distance between pixel values of both comparison windows surrounding the $\boldsymbol{p}$ and $\boldsymbol{q}$ pixels. Result of this is a scalar that tells us how similar the two neighborhoods around each pixel are. This process is then repeated for every other pixel in the search window around $\boldsymbol{p}$. The final value of $\boldsymbol{p}$ is then the average of all the pixels in the search window weighted by how similar each pixel is to pixel $\boldsymbol{p}$.

Chapter 5

Filtering evaluation methods

After the applying the filters on the noised images we need to evaluate how successful the filtration was which might be harder than it really sounds. Generally, evaluation methods can be divided into two groups, *subjective* methods and *objective* methods. In this thesis we will focus primarily on the objective methods as the main source of image filtration assessment. It is important to note that the best results are often achieved by the combination of both types of methods but sometimes we might be unable, for example due to logistics, utilize the subjective methods and make do only with the objective ones.

5.1 Subjective methods

The subjective methods are based on the fact that we can use our own sight to evaluate the quality of the images (hence the name subjective). The main advantage of this type of evaluation is the fact that, if done right, the results are tailored specifically to the future receivers of the image information, the people themselves. The obvious disadvantage of this lies in the fact that we need to form a large group of people, preferably of different ages, from different fields of expertise and different backgrounds altogether to create a reliable sample from which we can calculate e.g., the *Mean Opinion Score* (MOS) which was used in the past to evaluate the subjective quality of the audio transmissions in the telephone calls but can be repurposed for almost every subjective quality assessment [15].

5.2 Objective methods

The objective methods, which are the focus of this thesis, form the second group of quality assessment methods. These methods focus on evaluating the quality of an image based on mathematical methods and equations to calculate a certain score or index which is used to assess the quality of an image. As with subjective methods, even objective methods have their own advantages and disadvantages but the main problem but also benefit of this type of assessment is the lack of human bias. If done right, these methods

can provide us with a sort of a standardized scale on which we can simply evaluate an image based on a single number but at the same time it might not actually represent the reality well and an image with a good objective score might be subjectively of a very poor quality and not pleasant to look at.

When focusing on just the objective methods, we can further divide them into different subgroups based on the usage of the so-called *reference*. By doing this we can roughly construct 3 different groups [16].

5.2.1 Full reference methods

Full reference methods can give us a very accurate information about the quality of the assessed images because as a reference it uses the original image without any added noise. The main problem of these methods is already obvious. In holography we have no such thing as original image because the speckle noise present in the holographic images is there due to the nature of the holographic recording itself and thus there is no original image to be used as a reference. Despite this obvious big disadvantage, it might be valuable to use some of these methods even here in digital holography since some of the most used and known objective methods from the signal and image processing group belong to this very group, e.g., *Signal-to-noise ratio* (SNR), *Peak signal-to-noise ratio* (PSNR) *Structural similarity index measure* (SSIM) or *Mean squared error* (MSE). These methods are well-known and might serve as a sort of a steppingstone to a more advanced evaluation methods but due to the lack of the full reference, we might be forced to use these methods in a rather unconventional ways which might introduce us to a many new problems since these methods are not designed to be used without the full reference

MSE

Mean squared error is a very simple full reference method. It tells us the mean of the squared difference between the original and noised or otherwise distorted images as

$$MSE = \frac{1}{MN} \sum_{n_1=0}^{M-1} \sum_{n_2=0}^{N-1} [Y(n_1, n_2) - X(n_1, n_2)]^2, \tag{5.1}$$

where $Y(n_1, n_2)$ and $X(n_1, n_2)$ are the two evaluated images of the M×N size. This is the case for single channel grayscale image. For multiple channel RGB image we must make this calculation for every single channel and then make an average across all channels.[1]

PSNR

Signal-to-noise ratio is used as a ratio of the strength of the original signal (original image in this case) versus the strength of the noise on the background.

[1] RGB images usually have three different channels: red, green and blue.

Peak signal-to-noise is the ratio between the highest values of the signal and the noise. The easiest way to define PSNR is by the usage of MSE, which is explained above, as

$$PSNR = 10 \cdot \log_{10} \frac{MAX^2}{MSE} = 20 \cdot \log_{10} \frac{MAX}{\sqrt{MSE}}, \tag{5.2}$$

where MSE is the mean squared error and MAX is the maximal value of the pixel which is 255 for an 8-bit image, uint8 for short. If the image is RGB then we calculate PSNR for all 3 colors separately and then use the average of the 3 values as a final PSNR value. The PSNR is usually measured in *decibels* (dB), which is much more convenient because of the large dynamic range that the two compared signals, or holographic images in this case, might have.

SSIM

Structural similarity, SSIM for short, is used to compare the images based on the human perception of the image, which means it takes into consideration the psychovisual model of human vision [17]. The SSIM is based on 3 different characteristics: luminance, contrast and structure. First, we need to calculate a term for each of these characteristics. The final index is then a simple multiplicative combination of all three terms.

$$SSIM(x, y) = [l(x, y)]^{\alpha} \cdot [c(x, y)]^{\beta} \cdot [s(x, y)]^{\gamma}, \tag{5.3}$$

where α, β and γ are the weighting exponents. The three terms are then defined as

$$l(x, y) = \frac{2\mu_x\mu_y + C_1}{\mu_x^2 + \mu_y^2 + C_1}, \tag{5.4}$$

$$c(x, y) = \frac{2\sigma_x\sigma_y + C_2}{\sigma_x^2 + \sigma_y^2 + C_2}, \tag{5.5}$$

$$s(x, y) = \frac{\sigma_{xy} + C_3}{\sigma_x\sigma_y + C_3}, \tag{5.6}$$

where μ_x and μ_y are the local means, σ_x and σ_y are the standard deviations and σ_{xy} is the cross-covariance of the images x and y. The C_1, C_2 and C_3 are regularization constants which prevents undefined behavior in regions of the images where the local statistics might be near zero. By default (which also applies to this thesis) MATLAB calculates these as

$$C_1 = (0.01 \cdot MAX)^2, \tag{5.7}$$

$$C_2 = (0.03 \cdot MAX)^2, \tag{5.8}$$

$$C_3 = \frac{C_2}{2}, \tag{5.9}$$

where MAX is the dynamic range of the pixel, in this case its maximal value. When using the default settings and all exponential weights are equal to 1 then it all simplifies down to the one equation as

$$SSIM(x,y) = \frac{(2\mu_x\mu_y + C_1)\cdot(2\sigma_{xy} + C_2)}{(\mu_x^2 + \mu_y^2 + C_1)\cdot(\sigma_x^2 + \sigma_y^2 + C_2)}. \tag{5.10}$$

Range of the SSIM is then specified from -1 to 1, where 1 means the two input images are identical.

5.2.2 Reduced reference methods

Reduced reference methods are the compromise between full reference and no reference methods. One example of the reduced reference might me a low-resolution/downscaled version of the original image. This way we need less resources to transfer and process the reference image since the low-resolution version of the original image takes for example less memory. Quite obviously the results are then less accurate when compared to full reference, but we also saved some computational capacity. The reduced reference methods are not the focus of this thesis and therefore we continue to the other group of methods.

5.2.3 No-reference methods

No-reference objective methods are the focus of this thesis. In this case we have no original, noiseless image to work with, which is exactly the case of the digital holography, and therefore we must come up with new methods and algorithms of how to evaluate the quality of the used filters. The results of these methods might be less accurate than full reference or reduced reference methods, but in the end, they prove much more efficient because we need no original image to compare to. If done right the results of these methods are comparable even to the full-reference methods e.g., when we prove the validity of a certain no-reference method with the help of a subjective assessment done on a sufficient sample. One of the main goals of this thesis is to find the suitable no-reference methods which would be universally usable in the field of a digital holography with both the real recordings and *computer-generated* (CG) holograms. To this end a new method is being proposed called *Non-Local & Difference Variance Measure* (NLDVM) to address the problems of a missing full reference in the digital holography.

Non-Local & Difference Variance Measure (NLDVM)

Non-Local & Difference Variance Measure is a novelty experimental method, proposed by the author, to assess the quality of different filters in digital holography. It falls under the category of no-reference methods as it relies on a statistical approach, namely variance of the original noised image, variance of the filtered image and a variance of a *Noise map* which is a plain difference between the noised and noiseless image. In the sense of NLDVM we speak of

the variance of all the pixels in the image, not just in a small window, thus the name non-local. In this context original image means an image with speckle noise and not a noiseless reference and thus it is still a no-reference method. The original noised image is not even essential to the algorithm as it only serves as a normalization factor for the NLDVM to be more approachable with more easily comparable results.

The basis for this method is mainly the variance of the Noise map. The nature of the speckle noise is multiplicative so a plain difference between noised and filtered image does not provide us with an accurate measure of the speckle noise but that is not of concern in this case. The map M simply tells us which parts of the image were removed or altered during the filtration. The appearance of the map is very specific, and it depends on how successful the filtration was as seen in Figure 5.1 and Figure 5.2. We can clearly see that successful BM3D filtration removed the hologram noise while leaving the black areas as they were as seen by the very clear outlines in the Noise map. The NLM filtration, on the other hand, yielded much worse results as seen on the final image Y but also on the map itself. We cannot see any clear outlines of the hologram and the map looks almost blank. Such difference is sure to be represented in the variance of both images which is the reason why it is used in the NLDVM.

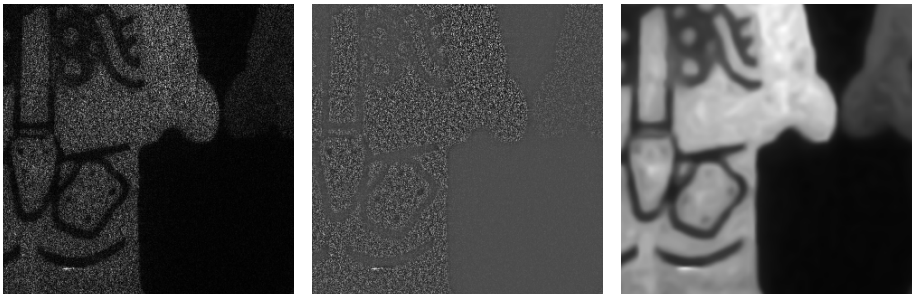

5.1.1 Hologram X 5.1.2 Noise map M 5.1.3 BM3D filtered Y

Figure 5.1: "Astronaut" hologram with BM3D filtering

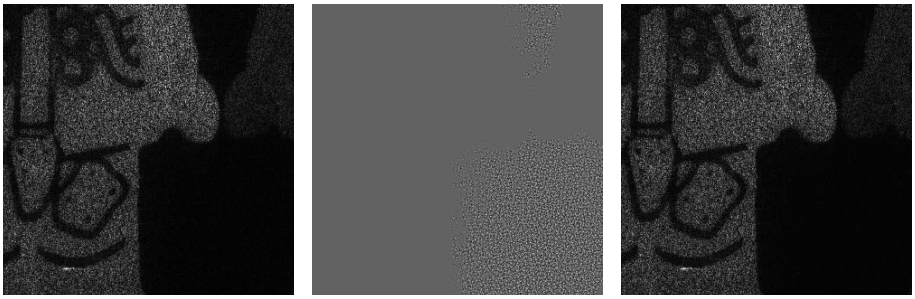

5.2.1 Hologram X 5.2.2 Noise map M 5.2.3 NLM filtered Y

Figure 5.2: "Astronaut" hologram with Non-Local Mean filtering

The variance of the Noise map itself would not give us precise results in all situations and thus it is multiplied with the variance of the filtered image Y. The reason for this is to prevent $NLDVM$ from being biased by overfiltering. If the images are overfiltered, the variance of the map will be high, as the hologram outlines would be much more clearly visible, which would be represented as good result, but the final image would be very distorted and subjectively not very good. While overfiltering would raise the variance of the map, it would also lower the variance of the final, filtered image. By multiplying these two variances, we keep the results balanced and unbiased to both the overfiltering and underfiltering.

The NLDVM is obtained as

$$NLDVM = (10^{-2b}) \cdot \mathrm{Var}[Y(n_1, n_2)] \cdot \mathrm{Var}[M(n_1, n_2)], \tag{5.11}$$

where Var is the function to obtain the variance and $M(n_1, n_2)$ is the Noise map obtained as

$$M(n_1, n_2) = X(n_1, n_2) - Y(n_1, n_2). \tag{5.12}$$

The exponent b is a normalization factor obtained from the variance of the original noised image as

$$\mathrm{Var}[X(n_1, n_2)] = a \cdot 10^b, \tag{5.13}$$

where a is the significand or coefficient of the variance of the original noised image $X(n_1, n_2)$ and b is the exponent. By combining all these together, we get the final equation as

$$\begin{aligned} NLDVM =& [10^{-2\log_{10}(\frac{\mathrm{Var}[X(n_1,n_2)]}{a})}] \cdot \mathrm{Var}[Y(n_1, n_2)] \cdot \\ & \cdot \mathrm{Var}[X(n_1, n_2) - Y(n_1, n_2)]. \end{aligned} \tag{5.14}$$

Non-Local & Difference Variance Measure per Computational Time

Computational complexity plays a big role in every filtration process. As seen above on the example of the BM3D filter, the results can be very good, but it says nothing about the time which the filtration took. In real world applications we must take into the account the quality/time ratio as even the best possible filter would be of little use if it took too long to process the image. Such concerns might become even more prominent in the future with the use of the digital holography for example in real time imaging. For such cases we need not the best filters but the filters with best quality/time ratio. That is the reason why we need to include the factor of time in the NLDVM method as

$$NLDVM_t = \frac{NLDVM}{time}, \tag{5.15}$$

where $NLDVM$ is divided by the *time* of the filtration. In this form the $NLDVM_t$ serves as another criterion we can use to determine the best-performing filter, specifically for the time-sensitive applications.[2]

[2] The computational time is dependent, e.g., on the settings or the used platform.

Part II

Practical part

Chapter 6

Experiment implementation

The aim of this thesis is not only to provide theoretical background of the speckle filtering and quality assessment methods in digital holography but to also demonstrate the said image processing methods in a practical implementation and to present the obtained results. For that end, an experiment is conducted and implemented in the MATLAB and discussed in this chapter with further results in the following chapter.[1]

6.1 Optical holographic images

To achieve the best possible accuracy of the filter assessment we need to use the real digital holographic data. For that purpose, the *EmergImg-HoloGrail-v2* databases of the project EmerImg by Marco V. Bernardo et al. [18] of the University of Beira Interior, Portugal, were used. The HoloGrail-v2 provides 6 different optically recorded digital holograms which can be used in additional experiments, like the filtration quality assessment, such as this. Holograms in these databases are in its raw form and need to be reconstructed first. The *Fresnel Impulse Response Method* (FIRM) is used to reconstruct these holograms, as described and implemented in MATLAB by authors of the holograms themselves [18].

6.2 Computer-generated holograms

Computer-generated holograms are holograms which were not created by the optical recording but, as the name suggests, computer-generated by the implementation of mathematical equations according to inserted model of a desired object. Another difference from the optical-recorded holograms is that these CG holograms do not suffer from the inherent speckle noise which is normally introduced in holograms due to the microscopic roughness of the recorded objects as the mathematical models which represents the objects can be considered "perfect". Thus, to work with these holograms we first need to introduce the speckle noise artificially as described in Eq. (3.2) in Chapter 3.4.

[1] MATLAB by MathWorks in version R2020a.

Why are the CG holograms needed

To evaluate how much useful the NLDVM is, it must be compared to other methods used in the field, namely PSNR, SSIM and MSE. The only problem is, as said above, is that these methods are full reference methods and thus not easily usable on the real holographic data obtained by optical recording. However, we can first evaluate the NLDVM performance on the computer-generated holograms where its results can be compared with the full reference methods. Because the speckle noise is introduced to these CG holograms artificially, we have both the noised image and the noiseless original image so the full reference methods are easily usable here and can help to determine the worth of the NLDVM.

6.3 MATLAB implementation

6.3.1 Filters

Some of the filters described above are already implemented in MATLAB but some more sophisticated filters like BM3D must be custom-implemented.

- BM3D filter was implemented in MATLAB by the authors Ymir Mäkinen et al. themselves [3].
- Frost filter was implemented by the MATLAB File Exchange user Debdoot Sheet and shared as a part of the MATLAB Central File Exchange [19].
- Lee filter was implemented by the MATLAB File Exchange user Grzegorz Mianowski and shared as a part of the MATLAB Central File Exchange [20].

Rest of the filters, i.e., Wiener filter, Box filter, Median filter and Non-Local Mean filter, are already implemented as base functions in MATLAB and its implementation can be found on the MathWorks MATLAB site.

In practical experiments was also used the *Lee & Frost* filter which is a simple combination of Lee filter and Frost filter as described above. The first stage of this filter is the preprocessing done by Lee filtration with its output being used as an input of the more robust Frost filter. It was chosen deliberately in this order. Since Frost filter is more sophisticated in its working, it changes the input pixels more than Lee filter would. This means that if the filters would be applied in order Frost-Lee, there might be no change at all when compared with the standalone Frost filter. However, this is the subjective view of the author since it was not tested in this reversed order.

6.3.2 Evaluation methods

NLDVM is implemented in MATLAB as a new function called `critVar(N,F)`. Its implementation can be observed in Listing 6.1.

Listing 6.1: The implementation of the NLDVM method in MATLAB

```
function var_crit = varCrit(noised,filtered)

map_filtered = noised - filtered;

% NLDVM = 10^[-2*log10(\Var[X]/a)]*\Var[Y]*\Var[X-Y]

var_crit = 10^(-2*(floor(log10(var(noised,0,'all'))))) * (
    var(filtered,0,'all') * var(map_filtered,0,'all'));

end
```

Other methods are already a native part of MATLAB as functions. Their implementations and used algorithms can be observed on the MATLAB MathWorks website.

- SSIM is implemented as `ssim(A,ref)` MATLAB function.
- PSNR is implemented as `psnr(A,ref)` MATLAB function.
- MSE is implemented as `immse(X,Y)` MATLAB function.

6.3.3 Fresnel Impulse Response Method

The Fresnel Impulse Response Method is already implemented in MATLAB by Marco V. Bernardo et al. [18], the authors of the EmergImg-HoloGrail-v2 database, for numerical reconstruction of their holograms. As seen in Listing 6.2, this method requires several inputs parameters. The most important are `pitch`, `lambda` and `z`.

- `pitch` is the pixel pitch or dot pitch, which is the distance from center of one pixel to the center of the adjacent pixel. For these holograms, the pixel pitch is 2.2 µm, while the LCD screens used today have pitch somewhere between 1 mm to 0.2 mm.
- `lambda` is the wavelength of the coherent light source used to record these holograms. The recording wavelength of the HoloGrail-v2 holograms is 632.8 nm.
- `z` is the propagation distance or reconstruction distance. It is the distance between the recording coherent light source and the recorded object. By the rules of the holography, it is also the distance at which the hologram is reconstructed.

The other inputs are `u1`, which is the recorded intensity pattern, `shiftx` and `shifty`, which are the shift parameters in horizontal X axis and vertical Y axis to center the hologram if needed and `signal`, which is the internal parameter set by the authors to determine if the used holograms are from the first of second version of their HoloGrail database and thus has no real value for the numerical reconstruction itself.

Listing 6.2: The implementation of the FIRM in MATLAB

```
%[u2] = propIR(u1,pitch,lambda,z,shiftx,shifty,signal);

k = 2*pi/lambda;
[M,N] = size(u1);

dx = pitch;
dy = pitch;
Lx = N*pitch;
Ly = M*pitch;
x = -Lx/2+shiftx*N*dx: dx : Lx/2+shiftx*N*dx-dx;
y = -Ly/2+shifty*M*dy: dy : Ly/2+shifty*M*dy-dy;

[X,Y] = meshgrid(x,y);

h = (-signal*1i)*exp((signal*1i*k/(2*z))*(X.^2+Y.^2));

U2=h.*u1;
u2=fftshift(ifft2(fftshift(U2)));
```

Scripts

The implementation of the whole experiment is included with this thesis in a form of MATLAB `.m` scripts archived in a `ZIP` repository. The full list of the included digital media, together with a README file, can be found in the Appendices in Chapter A.

Used hardware

The implementation was done on x64-based computer Dell Inc., Inspiron 15 7000 Gaming, CPU Intel(R) Core(TM) i7-7700HQ CPU @ 2.80GHz, 2801 MHz, supplemented by GPU NVIDIA GeForce GTX 1050 Ti and 16 GB RAM, utilized by MATLAB Parallel Computing Toolbox.

Chapter 7

Experiment results

Before assessing the quality of NLDVM method we need to create an appropriate computer-generated hologram for testing. However, since we are dealing with the reconstructed holograms in spatial domain in this experiment, as stated in the Chapter 1, using a real CG hologram would yield no true benefit. The numerical reconstruction of the CG hologram would be a simple 2-D image, no different from any other image or the source image, with the speckle noise added later, after the reconstruction.

7.1 CG hologram

For this purpose, an image in a `.png` format was used, once again the Hologram Earth by Kevin Gill. The picture was converted to grayscale `double` matrix and noised by MATLAB `imnoise()` function with speckle noise with the noise variance $\sigma^2 = 0.05$ as seen in Figure 7.1 where the effects of the speckle noise can be observed on a highlighted area selected from the image. The `imnoise()` function was used instead of the speckle noise model of Eq. (3.2) for easier reproducibility, with differences explained in Chapter 3.

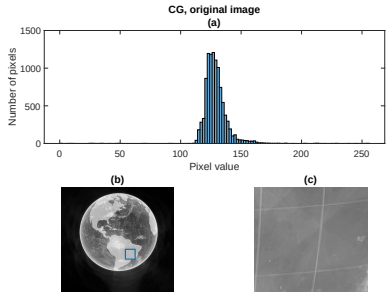

7.1.1 Original image

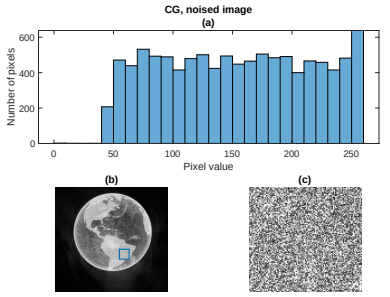

7.1.2 Image with speckle noise, $\sigma^2 = 0.05$

Figure 7.1: Image simulating the CG hologram, noised with speckle noise, (a) Histogram of the highlighted area, (b) Image, (c) Highlighted area

Whole image is then subjected to selected filters as seen in Figure 7.2 where the effects of the filtering can again be observed on a highlighted area complemented by a histogram of the highlighted area.

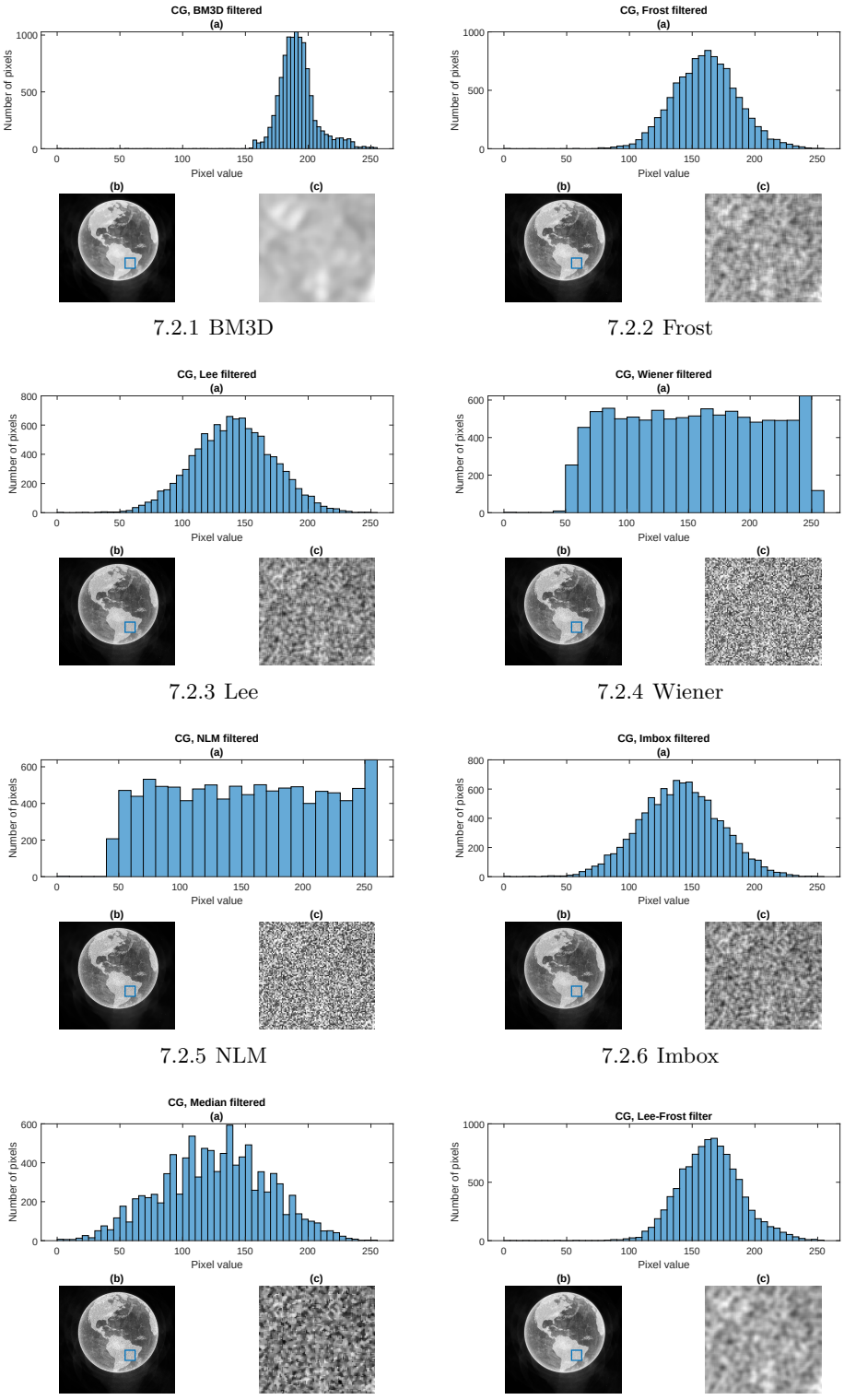

7.2.1 BM3D

7.2.2 Frost

7.2.3 Lee

7.2.4 Wiener

7.2.5 NLM

7.2.6 Imbox

7.2.7 Median

7.2.8 Lee-Frost

Figure 7.2: Speckle noise filtering on an image simulating a CG hologram, (a) Histogram of the highlighted area, (b) Image, (c) Highlighted area

These images are then complemented by the selected metrics, namely NLDVM, PSNR, SSIM and MSE as seen in Figure 7.3. The settings of the used filters, e.g., expected noise variance or local windows remains the same throughout the whole experiment. Corresponding values for the filter settings can be observed in Table 7.1.

Table 7.1: Used settings of the implemented filters on the CG hologram

CG hologram	
Filter	Settings (variance, window, ...)
BM3D	$\sigma^2 = 0.005$
Frost	M×N = 5×5
Lee	M×N = 3×3
Wiener	M×N = 5×5
Non-Local Mean	s: M×N = 29×29, c: M×N = 5×5
Imbox (2-D Box)	mean filter
Median	M×N = 3×3
Lee-Frost	L: M×N = 3×3, F: M×N = 5×5

According to the Full-reference (FR) methods PSNR and MSE, done on a single CG hologram, BM3D is pulling ahead with Frost, Lee-Frost, Imbox and Lee filters closely behind. When we take in account the psychovisual model of human vision and use SSIM methods, these same filters are still ahead but, in a different order. However, SSIM differences between almost all filters are rather insignificant. These results are complemented by histograms in Figure a 7.2 where it is easily observable that only these filters altered the histograms to a more expected state. Same result is seen on a histogram of the Median filter but according to FR methods, Median filter is slightly worse. However, NLDVM method also includes the Median filter along the five already mentioned filters, reflecting the change in the histogram. When looking at MSE, it can be observed that it just confirms the already mentioned findings with the highest errors in NLM and Wiener filters and the lowest error in BM3D filter.

Aside from the Median filter, the NLDVM method seems to be working just fine, promoting the good results of the filtering as seen with BM3D filter and strongly discouraging the bad filtration results, namely Wiener and NLM filter, just as other FR methods does.

It is also of interest to look at the results of the NLDVM_t. Imbox filter is pulling ahead of other filters rather significantly in terms of the quality/-time ratio with Median and Lee filters behind. Other used filters are either a low quality of simply take way too long to process and might be unfit for real-time digital holography processing in the foreseeable future. Fine example of this is the BM3D filter which is one of the best in terms of the quality of filtering, but its processing time is enormous when compared to other filters as seen in Figure 7.4.

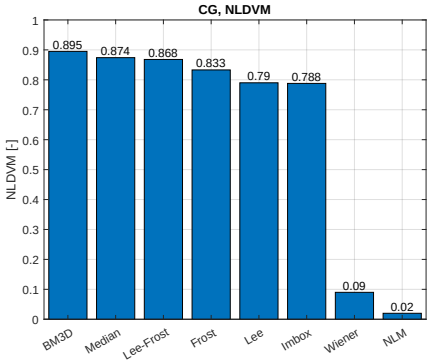

7.3.1 NLDVM

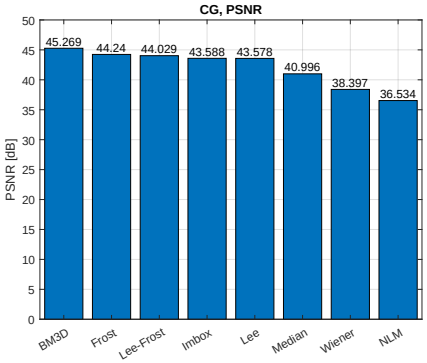

7.3.2 PSNR

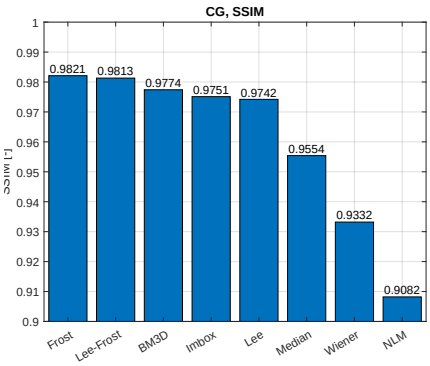

7.3.3 SSIM

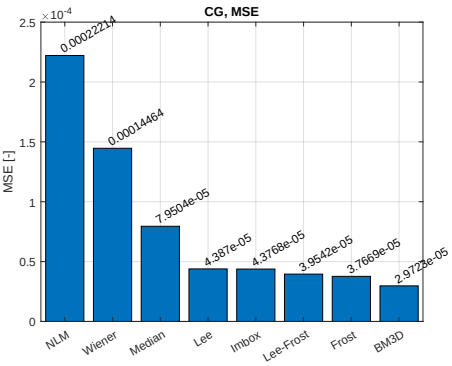

7.3.4 MSE

Figure 7.3: Used objective metrics to evaluate the filtration done on the CG hologram

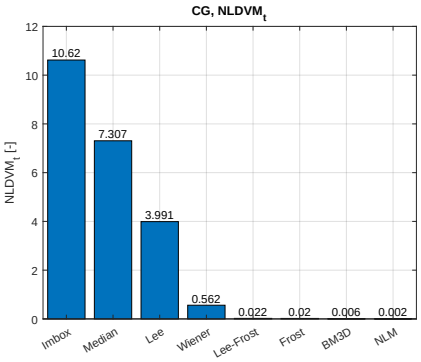

7.4.1 $NLDVM_t$

Computational time, CG hologram	
Filter	Time [s]
BM3D	149.93
Frost	41.8
Lee	0.20
Wiener	0.16
Non-Local Mean	10.49
Imbox (2-D Box)	0.07
Median	0.12
Lee-Frost	40.3

7.4.2 Computational time, CG hologram

Figure 7.4: Effects of the computational time on the NLDVM assessment method, CG hologram

- This part of the experiment, i.e., the simulated computer-generated hologram, is covered by the **b_generator_variables_cg.m** MATLAB script, see Chapter A for more info.

7.2 Optically recorded digital holograms

Now that we have a working method for hologram quality assessment, we can move on to the optically recorded holograms from the EmergImg-HoloGrail-v2 database and applying the selected filters on them. However, before moving on to the filtration itself, it might be useful to first select optimal settings for the filters. For CG holograms we used certain settings, but these might not be entirely optimal for real recordings. To find the optimal settings we need to plot the filter performance curves where on horizontal axis we have the settings value and on vertical axis we use a selected metric to assess the filter, NLDVM in this case.

7.2.1 Filter performance curves

To demonstrate the performance curves of the filters, BM3D, Wiener and NLM filters were chosen. Each of these filters use different settings, namely expected noise variance σ^2, local window of size M×N and search/compare windows sizes M×N. For other filters, the settings were chosen based on their performance on CG holograms mentioned above and default settings of the filters defined by authors of their implementations. All these curves were constructed on the optically recorded hologram "Astronaut" from the EmergImg-HoloGrail-v2 database.

BM3D filter

BM3D filter displayed exceptional filtering quality on CG holograms and thus it was the obvious first choice for performance curve. We can see in Figure 7.5 that the maximum performance of the filter is around the variance value $\sigma^2 = 0.35 \times 10^{-3}$, same for quality/time ratio with exception of occasional spikes caused by fluctuation in computational times.

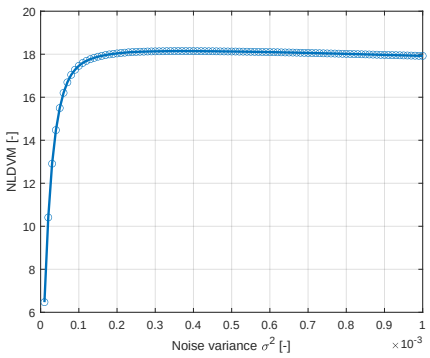

7.5.1 NLDVM curve of the BM3D filter

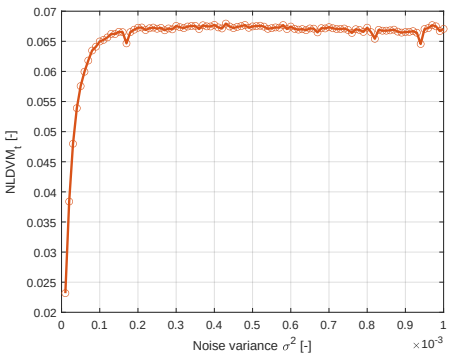

7.5.2 NLDVM$_t$ curve of the BM3D filter

Figure 7.5: BM3D filter performance curves using the NLDVM and NLDVM$_t$ methods, "Astronaut" hologram

After this value, the performance of the filters starts to drop. If we choose a more rough step on the horizontal axis and extend its range, we can clearly see an exponential decrease in the filter performance, so the top filter performance seems to be truly at expected noise variance value $\sigma^2 = 0.35 \times 10^{-3}$.

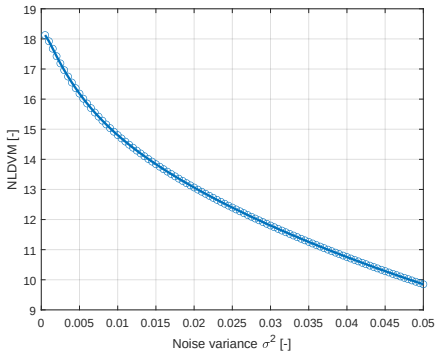

7.6.1 NLDVM curve of the BM3D filter

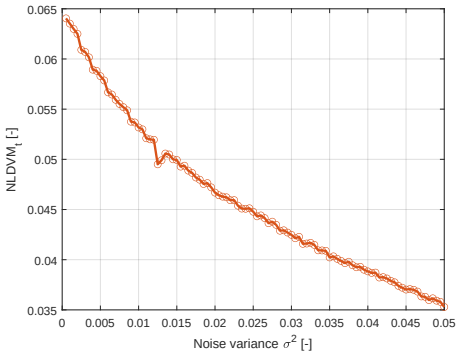

7.6.2 NLDVM$_t$ curve of the BM3D filter

Figure 7.6: BM3D filter performance curves using the NLDVM and NLDVM$_t$ methods with extended noise variance range, "Astronaut" hologram

Wiener filter

Wiener filter is a good example of a local-window-based filter and thus good for performance curve demonstration.

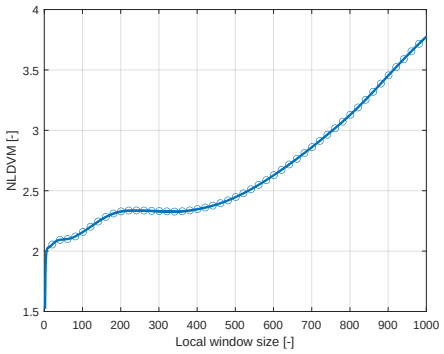

7.7.1 NLDVM curve of the Wiener filter

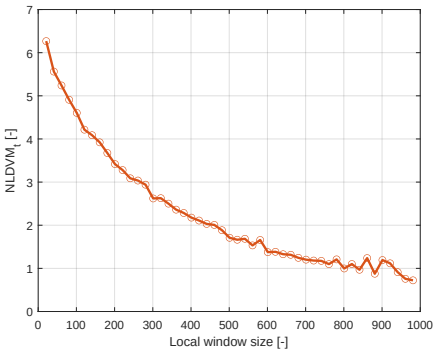

7.7.2 NLDVM$_t$ curve of the Wiener filter

Figure 7.7: Wiener filter performance curves using the NLDVM and NLDVM$_t$ methods, "Astronaut" hologram

Wiener filter seems to be increasing in quality with its window size growing but the size of the window is growing exponentially with based on the performance. To double the NLDVM the window size needs to be increased almost hundredfold to a rather ridiculous sizes 1000×1000 pixels. This fact is also projected into the quality/time ratio where we can see an exponential decrease in NLDVM$_t$ values thanks to the increasing computational time

which is connected to the size of the local window. Thus, it seems best to set the window reasonably small, somewhere between 5×5 to 10×10 pixels.

NLM filter

Optimizing the Non-Local Mean filter for best performance seems to be the most tricky of all the used filters since this filter uses two distinct windows to estimate the pixel values. To find the window size values for the best performance we need to use a 3-D scatter plot.

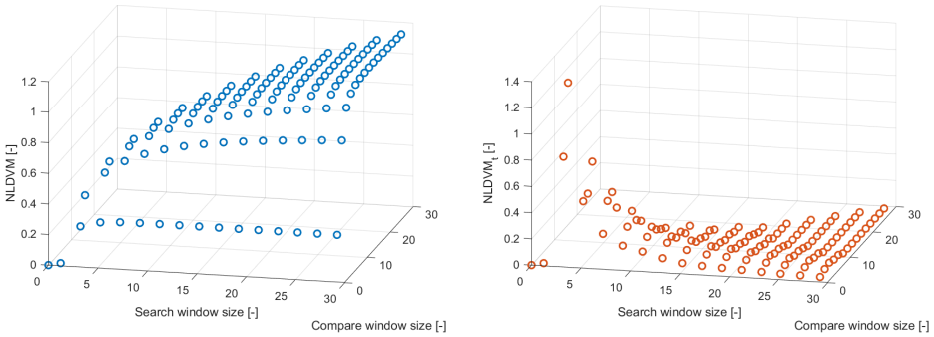

7.8.1 NLDVM curves of the NLM filter

7.8.2 NLDVM$_t$ curves of the NLM filter

Figure 7.8: NLM filter 3-D performance curves using the NLDVM and NLDVM$_t$ methods, "Astronaut" hologram

For both the search and compare windows, the curves are of a logarithmic nature but with a slight decrease for increasing window sizes. The best performance was achieved for search window with the size of 29×29 pixels complemented by compare window with the size of 5×5 pixels. Performance seems to be almost the same for bigger search window sizes and even decreasing for bigger compare windows. This is supported by the quality/time ratio of the filter measured in NLDVM$_t$, which is exponentially decreasing with the growing windows sizes.

- This part of the experiment, i.e., the filter performance curves, is covered by the **c_bm3d_wiener_curve.m** and **d_nlm_curve.m** MATLAB scripts, see Chapter A for more info.

7.2.2 Hologram resolution

Speaking of the sizes of the local windows it is worth mentioning the resolution of the recorded holograms. The size of the optically recorded and numerically reconstructed holograms in this experiment is 2588×2588 pixels. Notice the high resolution of the image. Such a high resolution is one of the inherent benefits of the digital holographic imaging even when used only as an amplitude part of the numerically reconstructed hologram, as is the case in this experiment.

7.2.3 Used filter settings

Once again, the settings of the used filters, e.g., expected noise variance or local windows remains the same throughout the whole experiment for all six holograms. Corresponding values for the filter settings can be observed in Table 7.2.

Table 7.2: Used settings of the implemented filters on the optically recorded digital holograms from the EmergImg-HoloGrail-v2 database

Optically recorded digital holograms	
Filter	Settings (variance, window, ...)
BM3D	$\sigma^2 = 0.001$
Frost	M×N = 5×5
Lee	M×N = 3×3
Wiener	M×N = 5×5
Non-Local Mean	s: M×N = 29×29, c: M×N = 5×5
Imbox (2-D Box)	mean filter
Median	M×N = 3×3
Lee-Frost	L: M×N = 3×3, F: M×N = 5×5

7.2.4 Used evaluation methods

When speaking of the assessment methods, main used method in the cases of the optically recorded holograms will be NLDVM but other mentioned methods might be of some use as well. In this case the PSNR, SSIM and MSE methods were also used but from "different" perspective. The filtered image was used instead of the noiseless reference and thus the scales of these methods were inverted meaning e.g., lower the PSNR or SSIM, the better. Scale of the MSE is also inverted meaning higher the MSE, better the image. When used like this, these methods, in fact, show a "distance" between the filtered and noised images. The main problem of this approach is that these methods were not primarily designed to be used this way and the results might be unreliable on their own.

Also take notice of the histograms of the highlighted areas of the holographic images. We will most likely see the clear dominance of the pixels on the left side of the scale, more to the darker tints. Apart from the NLDVM and other methods we can assess the image by the shape of the hologram and shift of the pixels to other parts of the scale, namely to the right side towards the center of the scale to the lighter tints

That being said, the main three assessment categories of the following images will be the NLDVM method, followed by the observation of the image histograms and lastly a subjective plain look of the author. FR methods will be used only to support the findings of other assessment methods. NLDVM_t method is only for a special use cases and thus will be handled separately.

7.2.5 Filtering results

Astronaut

With the "Astronaut" hologram, we have no full reference to compare the resulting filtered holographic images to, as seen in Figure 7.9. The full results of the filtering can be observed in Figure B.1 with assessment results in Figure C.1 and Figure C.2. The BM3D filter is once again pulling strongly ahead with Lee-Frost, Lee and Imbox filters behind, followed by Median and Frost filters. These findings are also supported by a plain look on the images and their respective histograms. As predicted, with these filters we can clearly see a shift to the right side of the histogram scale with a remaining spike in the darker tints due to the black lines which are part of the recorded object. From all the filters the results of the Frost filter are most surprising as it is the worst of these six best filters although the resulting image is, in fact, quite good when looked upon. That is however a subjective look of the author. This fact can also be used to justify the usage of the Lee and Frost filters together. The results of the Lee-Frost filter are very promising from all three perspectives, NLDVM, histogram and plain look. It is better than standalone Lee and Frost filters and ends up as the second-best filter right after BM3D while being significantly faster.

In the terms of the quality/time ratio, the Imbox filter is a clear winner. The filtering results are of a decent quality, but its computational time is unparalleled. For increase in quality, we might choose Lee or Median filter at the expense of a higher computational time, although still under one second.

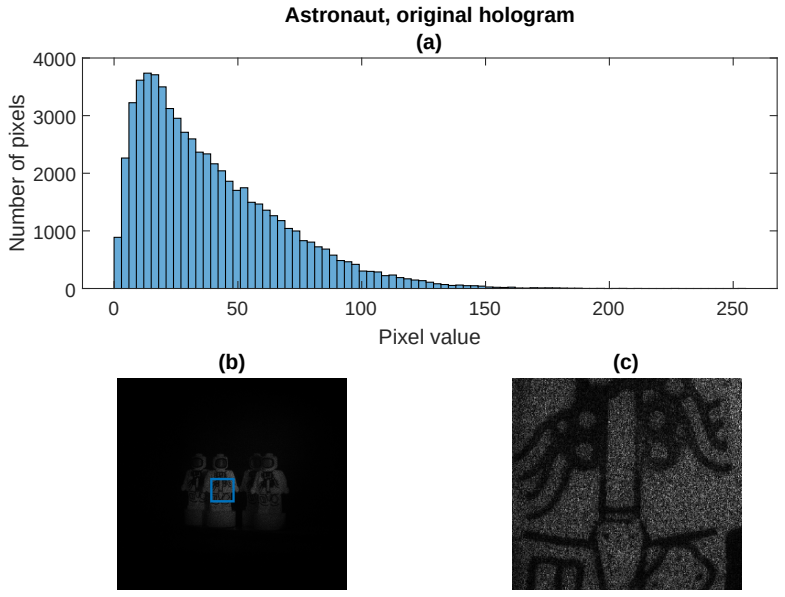

Figure 7.9: Speckle noise filtering on an optically recorded digital hologram "Astronaut", (a) Histogram of the highlighted area, (b) Image, (c) Highlighted area

Car

The original noised "Car" hologram image can be seen in Figure 7.10. The full results of the filtering can be observed in Figure B.2 with assessment results in Figure C.3 and Figure C.4. The BM3D filter once again proves as the best filter of all eight used filters, from the perspective of NLDVM, change in histogram shape and plain look. More lighter tints are starting to appear in the hologram due to the image smoothing and speckle noise suppression which results in the image brightening. BM3D filter is followed very closely by the Lee-Frost filter with both filters excelling in different areas. From the plain look and the theoretical design of these two filters, it can be observed that BM3D is very good at suppressing the speckle noise and smoothing the image while the Lee-Frost excels at edge preserving but at the cost of the slightly worse speckle noise suppression. These two filters are then followed by Median, Lee and Imbox with almost identical results in all three used assessment categories. Frost filter is once again last of the "better" filters, although author would subjectively put Frost filter results higher on the results but still after BM3D and especially the Lee-Frost filter, which seems to be working much better than a standalone Frost filter while retaining almost the same, in this case even lower, computational time.

In the terms of the quality/time ratio, the Imbox filter is once again a clear winner which is not at all surprising given the fact that it is by far the fastest filter of the filters used in this experiment. For increase in quality we, once again, might choose Lee or Median filter at the expense of a higher computational time, although still very fast, i.e., under one second.

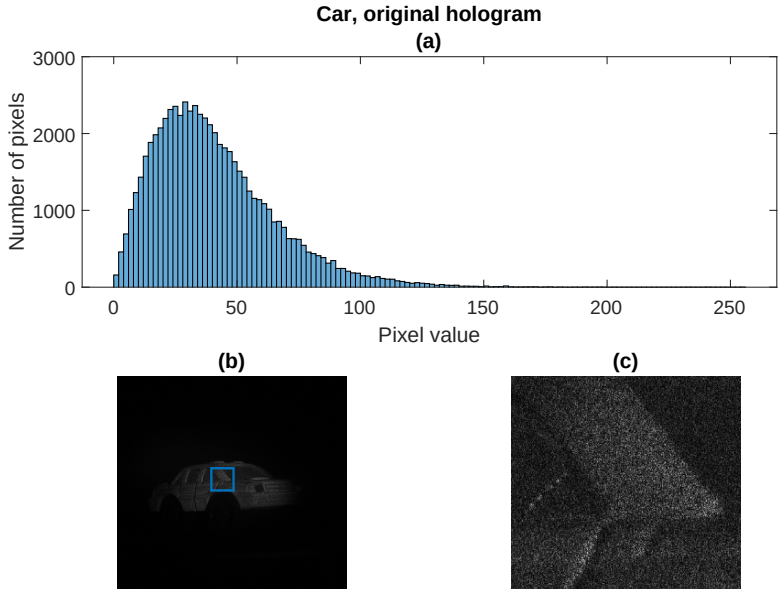

Figure 7.10: Speckle noise filtering on an optically recorded digital hologram "Car", (a) Histogram of the highlighted area, (b) Image, (c) Highlighted area

Dice1

The original noised "Dice1" hologram image can be seen in Figure 7.11. The full results of the filtering can be observed in Figure B.3 with assessment results in Figure C.5 and Figure C.6. The results of the NLDVM method are almost identical to the results of the hologram "Car" with BM3D pulling first, Lee-Frost behind, followed by Median, Lee and Imbox filters with almost the same NLDVM score and lastly the Frost filter. Wiener and NLM filters are once again behind other filters by a significant margin, confirmed by both the plain looks and their respective histograms which appear almost the same as the histogram of the original noised hologram. BM3D once again provides the superior noise suppression and smoothing at the expense of the worse edge preservation which is, on the other hand, the main quality of the Lee-Frost filter. Slight differences from the "Car" hologram can be seen with the FR methods, which seems to promote Median filter slightly more with BM3D filter still pulling strongly ahead, except for SSIM where the differences between each filter are in the order of magnitude of 10^{-3} to 10^{-2} and thus not very credible as a standalone assessment method.

In the terms of the quality/time ratio, the Imbox filter has a clear first spot, followed by the Median and Lee filters. These three filters together with Wiener filter are by far the fastest filters but Wiener lacks the quality of these three other fast filters.

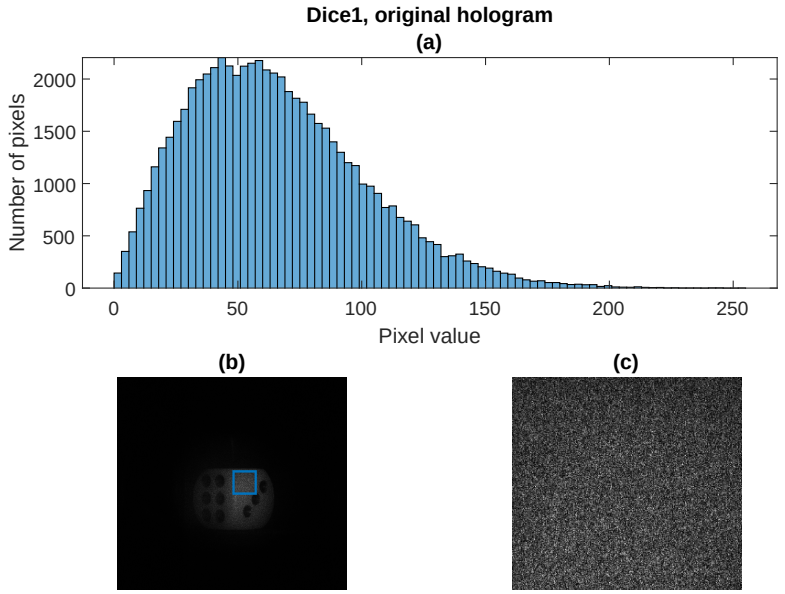

Figure 7.11: Speckle noise filtering on an optically recorded digital hologram "Dice1", (a) Histogram of the highlighted area, (b) Image, (c) Highlighted area

Dice2

The original noised "Dice2" hologram image can be seen in Figure 7.12. The full results of the filtering can be observed in Figure B.4 with assessment results in Figure C.7 and Figure C.8. There are not that many differences from the results of the "Dice1" hologram as the ranking of the filters is the same for all used metrics, even the quality/time ratio ranking of $NLDVM_t$ method is in the same order with the computational times being roughly the same to the "Dice1" hologram. The histograms are once again shifted more to the right towards the center of the histogram scale, which corresponds with the quality of the filtering, with most prominent change being once again visible in the histogram of the BM3D filtered hologram.

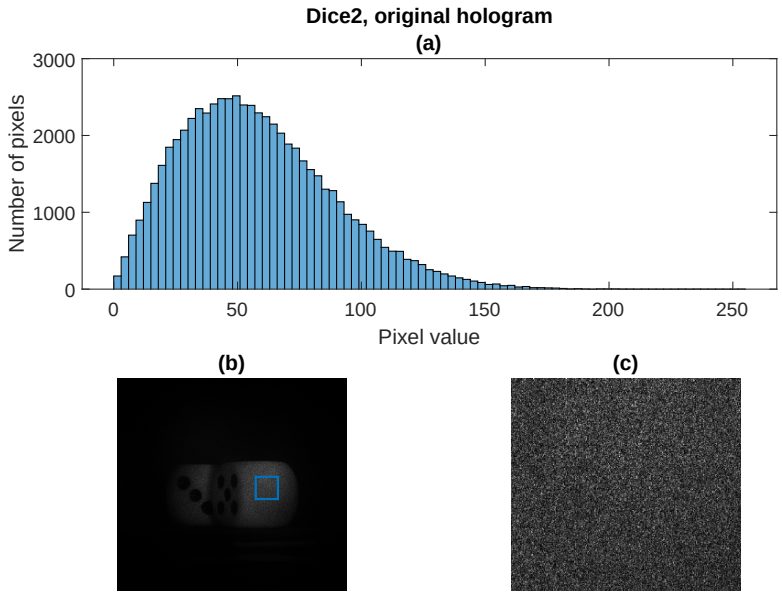

Figure 7.12: Speckle noise filtering on an optically recorded digital hologram "Dice2", (a) Histogram of the highlighted area, (b) Image, (c) Highlighted area

Chess

The original noised "Chess" hologram image can be seen in Figure 7.13. The full results of the filtering can be observed in Figure B.5 with assessment results in Figure C.9 and Figure C.10. Results are once again almost identical to the "Dice1" and "Dice2" holograms in terms of the NLDVM, PSNR and MSE. Very slight difference can be observed with the SSIM assessment method, where the ranking of the results is slightly different for the Lee, Imbox and Frost filters, with BM3D and Lee-Frost filters still being superior and Wiener and NLM filters being the worst of the used filters. However, the differences are again in the order of magnitude of 10^{-3} to 10^{-2} and thus not credible as a standalone assessment method. Histograms are once again shifted towards the center of the histogram scale due to smoothing, with BM3D filter being most prominent in this area as its histogram curve is different from the smooth, Gaussian-like histogram curves of the other filters, except for the Wiener and NLM filters. From the shapes of the BM3D histograms can be observed that this filter is truly the most complicated of all the used filters, as its histograms tend to have a "spiky", even discontinuous shape, with its discrete steps being more prominent when compared to the histograms of other filters used in this experiment. The ranking of the quality/time ratio of the $NLDVM_t$ method also remains the same as for both the "Dice1" and "Dice2" holograms.

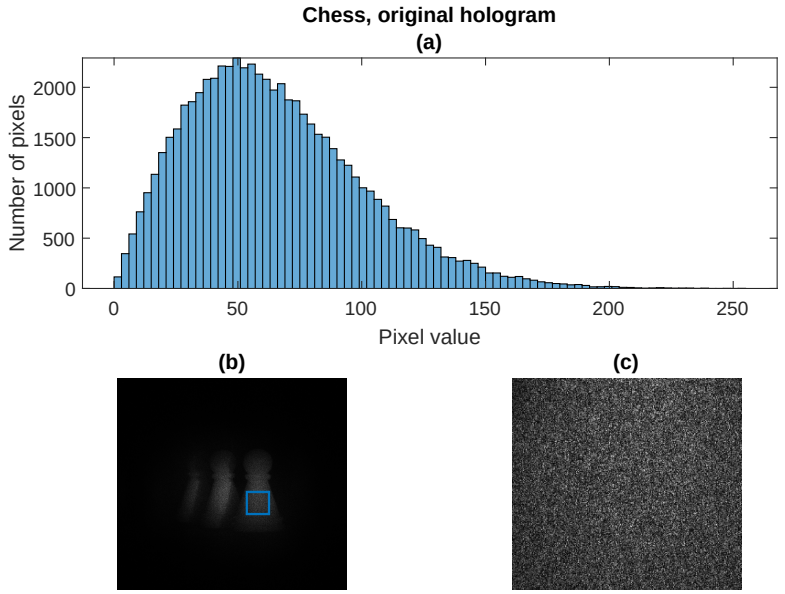

Figure 7.13: Speckle noise filtering on an optically recorded digital hologram "Chess", (a) Histogram of the highlighted area, (b) Image, (c) Highlighted area

Skull

The original noised "Skull" hologram image can be seen in Figure 7.14. The full results of the filtering can be observed in Figure B.6 with assessment results in Figure C.11 and Figure C.12. Even the "Skull" hologram has no significant difference to the previous holograms like "Dice1", "Dice2" or "Chess". Histograms are also once again shifted towards the center of the histogram scale with most noticeable changes being with the BM3D histogram. The ranking of the quality/time ratio of the NLDVM_t method remains the same as for the previous holograms.

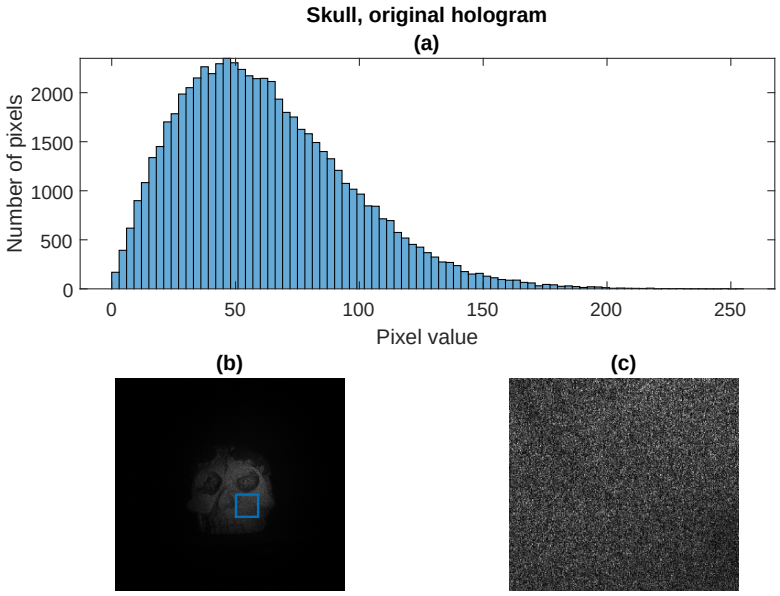

Figure 7.14: Speckle noise filtering on an optically recorded digital hologram "Skull", (a) Histogram of the highlighted area, (b) Image, (c) Highlighted area

- This part of the experiment, i.e., all six optically recorded holograms, is covered by the **a_generator_variables_optical.m** MATLAB script, see Chapter A for more info.

7.3 Final results

Overall ranking of the filters for each holographic image can be observed in the Table 7.3. The results of the experiment are quite clear. BM3D filter proved to be the best speckle-suppressing filter of all the filters used in this experiment, followed the Lee-Frost which is slightly worse in speckle noise suppression but offers a better edge preservation when compared to BM3D filter. Lee-Frost filter is also almost 30% faster in average computational time when compared to the BM3D, as can be observed in Figure 7.16. Ranking of all the used filters is in Figure 7.15. A NLDVM-based *Score* was calculated for each filter as

$$Score = R \cdot Average_{filter}(NLDVM), \tag{7.1}$$

where $Average_{filter}(NLDVM)$ is the average NLDVM per filter across all six holographic images and R is a rate calculated from the Table 7.3. Each filter gets a specific number of points based on its place in the table, e.g., for "Astronaut" hologram, BM3D filter is in the first place, so it is awarded 8 points, Lee-Frost ended up second, so it gets 7 points and so on. Points are then summed up across all six holograms.[1]

Table 7.3: Filter ranking based on the NLDVM

Filter quality ranking based on the NLDVM								
Hologram	1^{st}	2^{nd}	3^{rd}	4^{th}	5^{th}	6^{th}	7^{th}	8^{th}
CG	BM3D	Median	Lee-Frost	Frost	Lee	Imbox	Wiener	NLM
Astronaut	BM3D	Lee-Frost	Lee	Imbox	Median	Frost	Wiener	NLM
Car	BM3D	Lee-Frost	Median	Lee	Imbox	Frost	Wiener	NLM
Dice1	BM3D	Lee-Frost	Median	Lee	Imbox	Frost	Wiener	NLM
Dice2	BM3D	Lee-Frost	Median	Lee	Imbox	Frost	Wiener	NLM
Chess	BM3D	Lee-Frost	Median	Lee	Imbox	Frost	Wiener	NLM
Skull	BM3D	Lee-Frost	Median	Lee	Imbox	Frost	Wiener	NLM

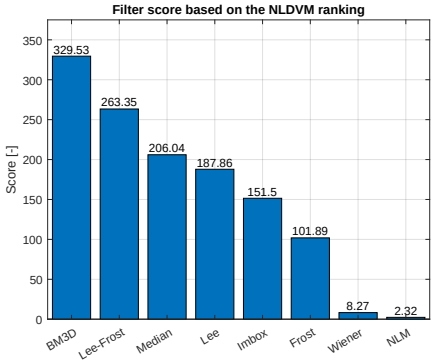

7.15.1 NLDVM-based score graph

Final filter score		
Filter	Score	R
BM3D	329.53	48
Lee-Frost	263.35	42
Median	206.04	34
Lee	187.86	31
Imbox (2-D Box)	151.50	25
Frost	101.89	18
Wiener	8.27	12
Non-Local Mean	2.32	6

7.15.2 NLDVM-based score table

Figure 7.15: Filter score based on the NLDVM ranking for the optically recorded holograms

[1] The CG hologram is omitted from this score as it was used only to test the NLDVM method.

Since the NLDVM method normalizes the results for each holographic image individually, it is of little value to compare just the plain NLDVM values for the same filter across different images. This is the reason why the average NLDVM per filter across all holographic images is scaled by the R value.

Quality/time ratio

In terms of the quality/time ratio measured by the NLDVM_t method, Imbox filter is a clear winner across all six holographic images with an unparalleled computational time, as seen in Figure 7.16, followed by the Median and Lee filters. Median and Lee filters offer higher image quality, for a price of almost a 6× higher computational time in case of the Lee filter, when compared to the Imbox filter. But even then, the average computational time is under one second for a high-resolution image of 2588×2588 pixel, which is still very good. Imbox, Median and Lee filters are highly suitable for time-sensitive holographic imaging and image processing applications with the certain quality trade-offs, depending on the application. Full results can be observed in the Table 7.4.

Table 7.4: Filter ranking based on the NLDVM_t

Filter quality/time ratio ranking based on the NLDVM_t								
Hologram	1^{st}	2^{nd}	3^{rd}	4^{th}	5^{th}	6^{th}	7^{th}	8^{th}
CG	Imbox	Median	Lee	Wiener	Lee-Frost	Frost	BM3D	NLM
Astronaut	Imbox	Lee	Median	Wiener	Lee-Frost	Frost	BM3D	NLM
Car	Imbox	Median	Lee	Wiener	Lee-Frost	Frost	NLM	BM3D
Dice1	Imbox	Median	Lee	Wiener	Lee-Frost	Frost	BM3D	NLM
Dice2	Imbox	Median	Lee	Wiener	Lee-Frost	Frost	BM3D	NLM
Chess	Imbox	Median	Lee	Wiener	Lee-Frost	Frost	BM3D	NLM
Skull	Imbox	Median	Lee	Wiener	Lee-Frost	Frost	BM3D	NLM

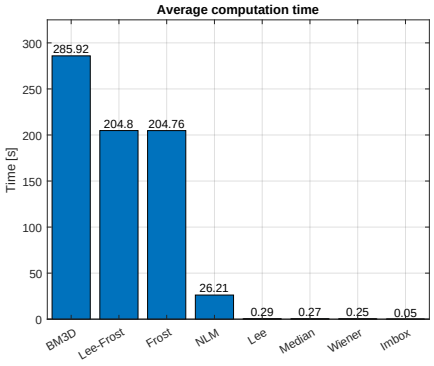

7.16.1 Average computational time graph

Average computational time	
Filter	Time [s]
BM3D	285.92
Lee-Frost	204.80
Frost	204.76
Non-Local Mean	26.21
Lee	0.29
Median	0.27
Wiener	0.25
Imbox (2-D Box)	0.05

7.16.2 Average computational time table

Figure 7.16: Average computational time for the optically recorded holograms

Chapter 8

Conclusion

In the first, theoretical, part of this work, an overview of the field of the digital holography and its inherent speckle noise is given, while primary focused on the image filtering techniques and the objective evaluation methods to assess the quality of the said filtering techniques. It is also in this part where the new objective evaluation method called NLDVM is being proposed, to address one of the main challenges of the objective filtering quality evaluation in this field, which is the absence of the reference image and thus the inability to use the well-known Full-reference evaluation methods like PSNR, SSIM or MSE.

In the second, practical part, an implementation of an experiment is first discussed while the experiment itself is then conducted in the MATLAB environment. This experiment implements the filtering techniques discussed in the first part and applies them in the spatial, image domain on a set of numerically reconstructed holograms obtained by an optical recording of real objects. It is also here that a new type of filter called Lee-Frost is being proposed, which is a plain combination of the Lee and Frost filtering techniques. Afterwards, the proposed objective evaluation methods are also implemented and applied on the filtered holographic images, including the new NLDVM method, which is also used in an altered form to address the commercial side of things with the quality/time ratio and time-sensitivity of the said filtering techniques in mind.

The NLDVM method seems to perform well which is proved in a test conducted as a part of the experiment itself, where NLDVM was used on par with the Full-reference methods PSNR, SSIM and MSE and yielded the same results. The proposed new method is then being used as a main objective evaluation method for the rest of the experiment.

The results of the experiment revealed that the BM3D filter is the best performing filter for the specified use case and selected conditions, when it comes to the quality. However, the price is paid heavily by the large computational time. This filter is closely followed by the proposed Lee-Frost filter, which is performing better than the standalone Lee and Frost filters, while being just as fast as the Frost filter. Other filters, namely Median, Lee,

Imbox and Frost are following with similar results. And lastly, the Wiener and NLM filters seems to have little to no effect on the holographic images, which is projected in the final score, their respective histograms and also clearly visible by a plain look.

In terms of quality/time ratio measured by the altered NLDVM method called NLDVM_t, the Imbox filter, set as mean filter, is a clear winner in the quality/time ratio for the selected conditions and seems to be well fit for the time-sensitive applications with an expected trade-off in quality. Substitute for the Imbox filter are the Lee and Median filters, which both offer higher quality results when compared to the Imbox filter but at the expense of a higher computational time. Even with the better quality, these filters are still quite fast with the average computational time being lower than one third of a second and thus making them valuable for time-sensitive applications. However, for some theoretical high-resolution holographic applications like video recording, which might be considered in the near future, the Imbox filter is still a superior choice since it is on average 5 to 6 times faster than the Lee or Median filters, while the quality difference is not that high.

In future experiments, there are a few things to be considered. In this work, the proposed NLDVM method was tested only on a single simulated CG hologram before being used on the optically recorded holograms. It might be of worth to test this method on multiple holograms, either CG or optically recorded. However, to properly test this method, it would be suitable to pair its objective results with the results from a subjective test performed on a big enough sample. Another thing, which might be improved, are the filter settings. In the conducted experiment, the settings of the used filters remained the same for all optically recorded holograms. It is unlikely that the final ranking of the used filters would change drastically, but it is still a thing to be considered for the future. However, it might have a noticeable impact on the quality/time ratio ranking of the used filters, since the computational time is proportional to the used settings for several filters used in this experiment, as seen earlier in this Chapter in Filter performance curves section. These curves could also be supplemented by other performance curves, measured in PSNR or SSIM, on the CG holograms, to better show the difference or rather the similarity of these curves and the NLDVM curve.

Bibliography

[1] G. Cristóbal, P. Schelkens, and H. Thienpont, *Optical and digital image processing: fundamentals and applications*. Wiley-VCH GmbH & Co, April 2011. Online; https://doi.org/10.1002/9783527635245; ISBN: 9783527635245; accessed 20 January 2020.

[2] O. Faragallah, H. Elhoseny, W. El-Shafai, W. El-Rahman, H. El-sayed, E.-S. El-Rabaie, F. Abd El-Samie, and G. Geweid, "A Comprehensive Survey Analysis for Present Solutions of Medical Image Fusion and Future Directions," *IEEE Access*, vol. 9, December 2020. Online; https://dx.doi.org/10.1109/ACCESS.2020.3048315; accessed 27 April 2021.

[3] Y. Mäkinen, L. Azzari, and A. Foi, "Collaborative Filtering of Correlated Noise: Exact Transform-Domain Variance for Improved Shrinkage and Patch Matching," *IEEE Transactions on Image Processing*, vol. 29, August 2020. Online; https://doi.org/10.1109/TIP.2020.3014721; accessed 29 March 2021.

[4] P. Schelkens, T. Ebrahimi, A. Gilles, P. Gioia, K. Oh, F. Pereira, C. Perra, and A. M. G. Pinheiro, "JPEG Pleno: Providing representation interoperability for holographic applications and devices," *ETRI Journal*, vol. 41, p. 93–108, February 2019. Online; https://doi.org/10.4218/etrij.2018-0509; accessed 10 April 2021.

[5] E. Fonseca, P. T. Fiadeiro, M. V. Bernardo, A. Pinheiro, and M. Pereira, "Assessment of speckle denoising filters for digital holography using subjective and objective evaluation models," *Applied Optics*, vol. 58, pp. 282–292, December 2019. Online; https://doi.org/10.1364/AO.58.00G282; accessed 10 April 2021.

[6] S. W. Hasinoff, "Photon, Poisson Noise," *Computer Vision*, p. 608–610, February 2016. Online; https://doi.org/10.1007/978-0-387-31439-6_482; accessed 30 January 2020.

[7] J. Jaybhay and R. Shastri, "A Study of Speckle Noise Reduction Filters," *Signal & Image Processing An International Journal*, vol. 6, pp. 71–80, June 2015. Online; https://dx.doi.org/10.5121/sipij.2015.6306; accessed 11 May 2021.

[8] V. Bianco, P. Memmolo, M. Leo, S. Montresor, C. Distante, M. Paturzo, P. Picart, B. Javidi, and P. Ferraro, "Strategies for reducing speckle noise in digital holography," *Nature News*, August 2018. Online; https://doi.org/10.1038/s41377-018-0050-9; accessed 20 January 2020.

[9] P. Singh and R. Pandey, "Speckle noise: Modelling and implementation," *International Journal of Circuit Theory and Applications*, vol. 9, pp. 8717–8727, January 2016. Online; https://www.researchgate.net/publication/312061215_Speckle_noise_Modelling_and_implementation; accessed 07 February 2020.

[10] K. Gill, "Hologram Earth," August 2014. Online; https://www.flickr.com/photos/kevinmgill/14676390490/in/photostream/; accessed 19 April 2021, licensed under CC BY 2.0.

[11] J. S. Lim, "Two-Dimensional Signal and Image Processing," *Englewood Cliffs, N.J., Prentice Hall*, pp. 548, eq. 9.44, 9.45 and 9.46, September 1989. ISBN: 9780139353222; accessed 09 May 2021.

[12] V. S. Frost, J. A. Stiles, K. S. Shanmugan, and J. C. Holtzman, "A Model for Radar Images and Its Application to Adaptive Digital Filtering of Multiplicative Noise," *IEEE Transactions on Pattern Analysis and Machine Intelligence*, vol. PAMI-4, pp. 157–166, March 1982. Online; https://dx.doi.org/10.1109/TPAMI.1982.4767223; accessed 02 April 2021.

[13] J. S. Lee, "Digital Image Enhancement and Noise Filtering by Use of Local Statistics," *IEEE Transactions on Pattern Analysis and Machine Intelligence*, vol. PAMI-2, pp. 165–168, March 1980. Online; https://dx.doi.org/10.1109/TPAMI.1980.4766994; accessed 04 April 2021.

[14] A. Buades, B. Coll, and J.-M. Morel, "Non-Local Means Denoising," *Image Processing On Line*, vol. 1, September 2011. Online; https://doi.org/10.5201/ipol.2011.bcm_nlm; accessed 31 March 2021.

[15] P. Ye and D. Doermann, "Active Sampling for Subjective Image Quality Assessment," *2014 IEEE Conference on Computer Vision and Pattern Recognition*, pp. 4249–4256, June 2014. Online; https://dx.doi.org/10.1109/CVPR.2014.541; ISBN: 9781479951185; accessed 11 May 2021.

[16] Z. Wang, "Applications of Objective Image Quality Assessment Methods," *IEEE Signal Processing Magazine*, vol. 28, pp. 137–142, November 2011. Online; https://dx.doi.org/10.1109/MSP.2011.942295; accessed 11 May 2021.

[17] Z. Wang, A. Bovik, H. Sheikh, and E. Simoncelli, "Image quality assessment: from error visibility to structural similarity," *IEEE Transactions on Image Processing*, vol. 13, pp. 600–612, April 2004. Online; https://dx.doi.org/10.1109/TIP.2003.819861; accessed 09 May 2021.

[18] M. V. Bernardo, P. Fernandes, A. Arrifano, M. Antonini, E. Fonseca, P. T. Fiadeiro, A. M. Pinheiro, and M. Pereira, "Holographic representation: Hologram plane vs. object plane," *Signal Processing: Image Communication*, vol. 68, pp. 193–206, October 2018. Online; `https://doi.org/10.1016/j.image.2018.08.006`; accessed 10 April 2021.

[19] D. Sheet, "Frost's Filter," *MATLAB Central File Exchange*, February 2012. Online; `https://www.mathworks.com/matlabcentral/fileexchange/35073-frost-s-filter`; accessed 10 April 2021.

[20] G. Mianowski, "Lee filter," *MATLAB Central File Exchange*, June 2010. Online; `https://www.mathworks.com/matlabcentral/fileexchange/28046-lee-filter`; accessed 10 April 2021.

Appendices

Appendix A

Included digital media

Custom MATLAB scripts

- **a_generator_variables_optical.m** → Script for generating and displaying all the necessary variables for the experiment with the optically recorded holograms in a `.pdf` format.
- **b_generator_variables_cg.m** → Script for generating and displaying all the necessary variables for the experiment with the simulation of the CG hologram in a `.pdf` format.
- **c_bm3d_wiener_curve.m** → Script for generating the performance curves of the BM3D and Wiener image filters.
- **d_nlm_curve.m** → Script for generating the performance curves of the Non-Local Mean image filter.
- **e_generator_png.m** → Script for generating the holographic images in a `.png` format.
- **f_generator_map.m** → Script for generating the holographic Noise maps in a `.png` format.
- **histoBorder.m** → Custom MATLAB function necessary for the correct behavior of other displaying scripts.
- **varCrit.m** → Custom MATLAB function with the implemented NLDVM objective evaluation method.

Other MATLAB scripts, e.g., from other authors

- **fcnFrostFilter.m** → Script with the Frost image filter.
- **myLee.m** → Script with the Lee image filter.
- **propIR.m** → Script for the numerical reconstruction of the optically recorded digital holograms using the FIRM method.
- **bm3d_matlab_package** → Folder with scripts needed for the functional BM3D filter implementation.

Images

- **earth.jpg** → Image in a `.jpg` format used for the CG hologram simulation, Hologram Earth by Kevin Gill under *CC BY 2.0*, modified.

Others

- **README.pdf** → README file.

All the digital media are contained in a `ZIP` repository, which is included with this thesis.

Custom scripts included in this thesis were created in the version R2020a of the MATLAB environment. Other used scripts are also compatible with this version.

Holograms from the EmergImg-HoloGrail-v2 databases, used in these scripts, are not included. Download from:

- `http://emergimg.di.ubi.pt/index.html`

The original image Hologram Earth by Kevin Gill under *CC BY 2.0* is not included. Download from:

- `https://www.flickr.com/photos/kevinmgill/14676390490/`

Appendix B

Optically recorded holograms, filtered

Astronaut

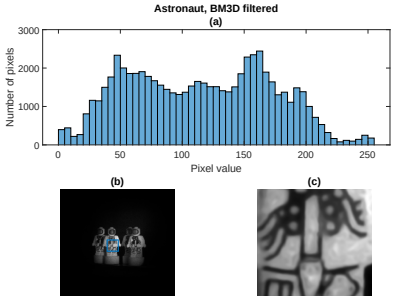

B.1.1 BM3D

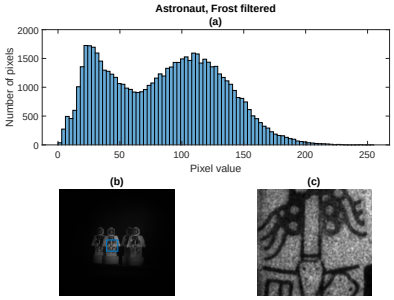

B.1.2 Frost

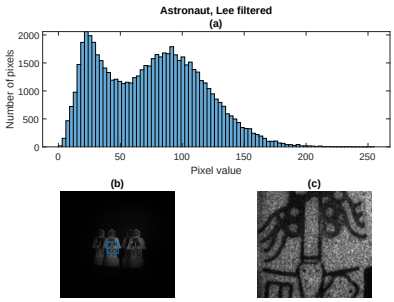

B.1.3 Lee

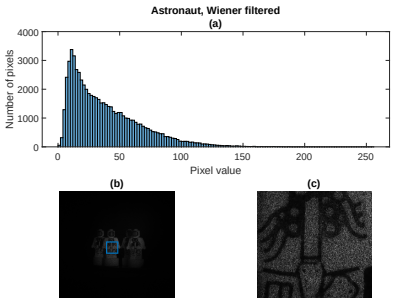

B.1.4 Wiener

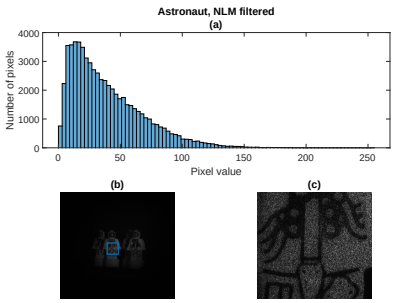

B.1.5 NLM

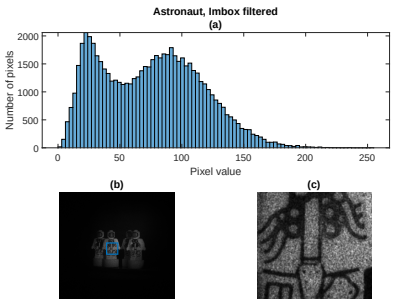

B.1.6 Imbox

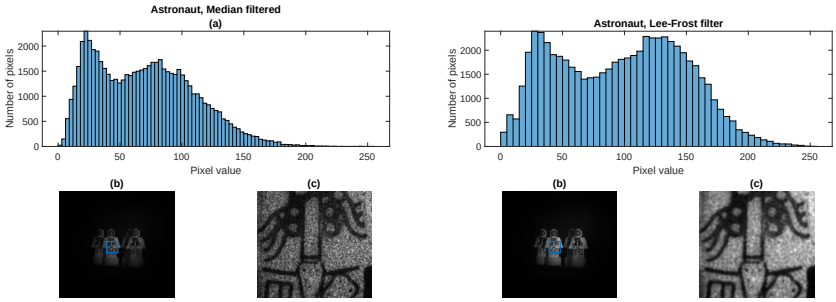

B.1.7 Median B.1.8 Lee-Frost

Figure B.1: Speckle noise filtering on an optically recorded digital hologram "Astronaut", (a) Histogram of the highlighted area, (b) Image, (c) Highlighted area

Car

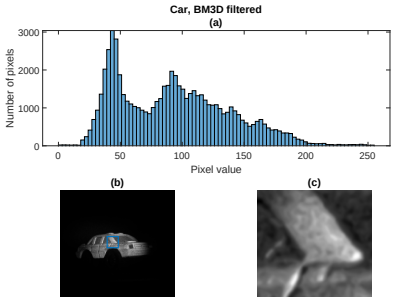

B.2.1 BM3D

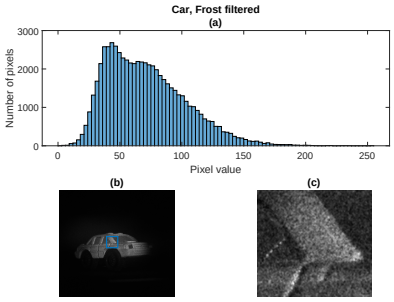

B.2.2 Frost

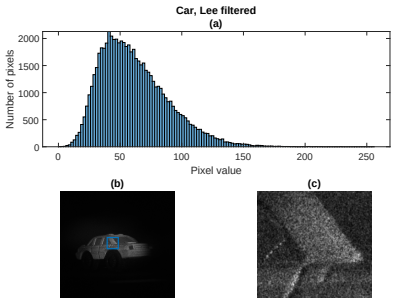

B.2.3 Lee

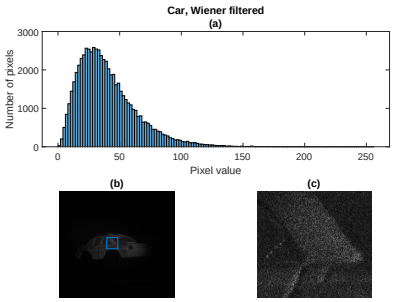

B.2.4 Wiener

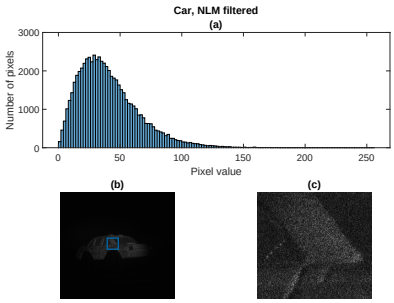

B.2.5 NLM

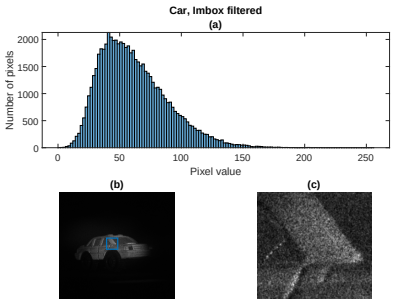

B.2.6 Imbox

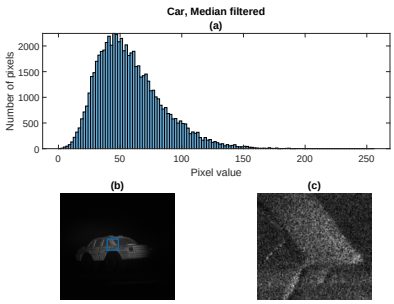

B.2.7 Median

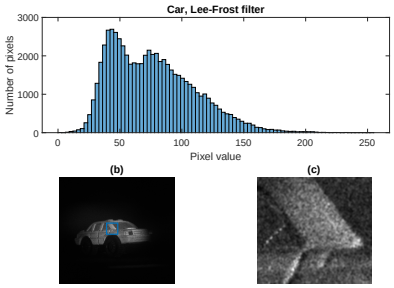

B.2.8 Lee-Frost

Figure B.2: Speckle noise filtering on an optically recorded digital hologram "Car", (a) Histogram of the highlighted area, (b) Image, (c) Highlighted area

Dice1

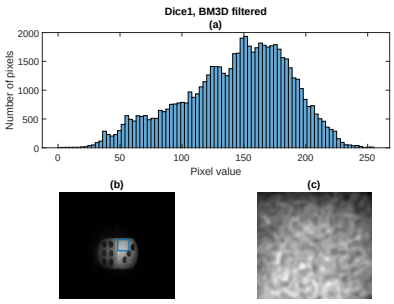

B.3.1 BM3D

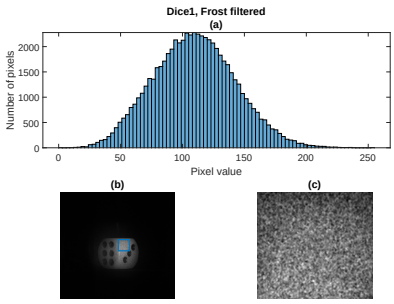

B.3.2 Frost

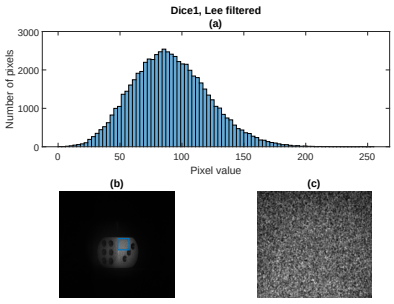

B.3.3 Lee

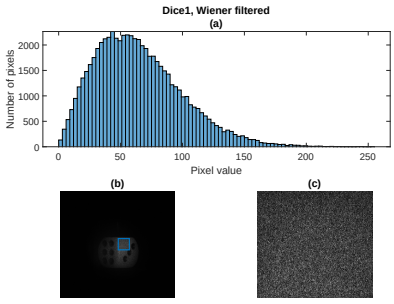

B.3.4 Wiener

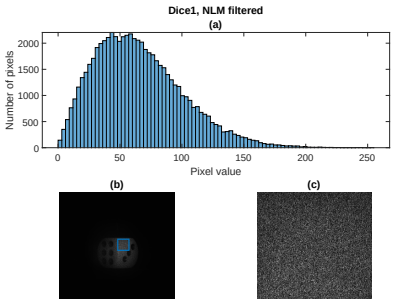

B.3.5 NLM

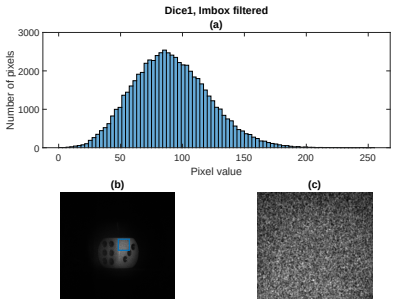

B.3.6 Imbox

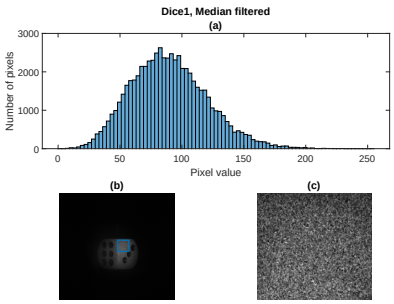

B.3.7 Median

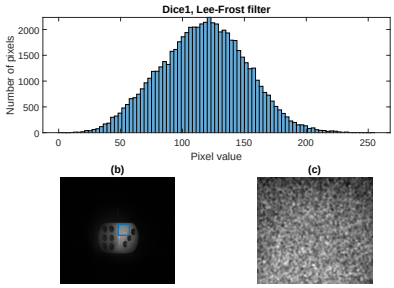

B.3.8 Lee-Frost

Figure B.3: Speckle noise filtering on an optically recorded digital hologram "Dice1", (a) Histogram of the highlighted area, (b) Image, (c) Highlighted area

Dice2

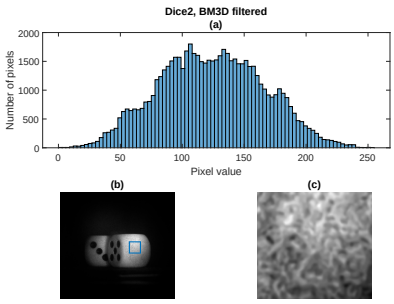

B.4.1 BM3D

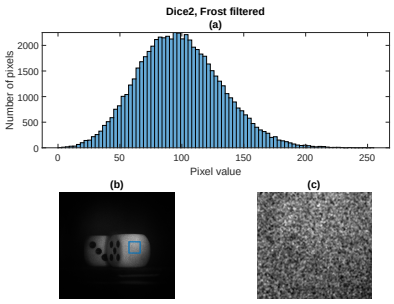

B.4.2 Frost

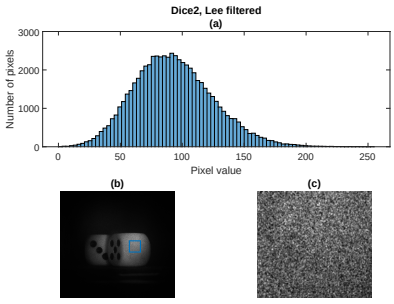

B.4.3 Lee

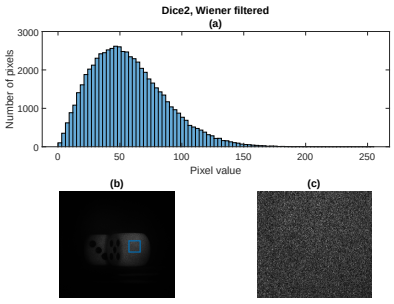

B.4.4 Wiener

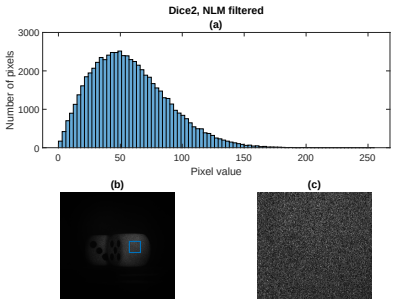

B.4.5 NLM

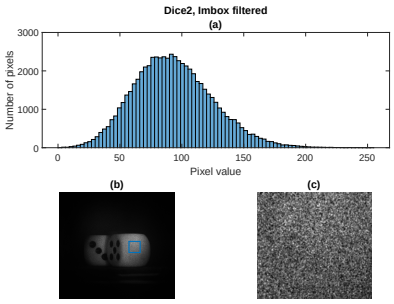

B.4.6 Imbox

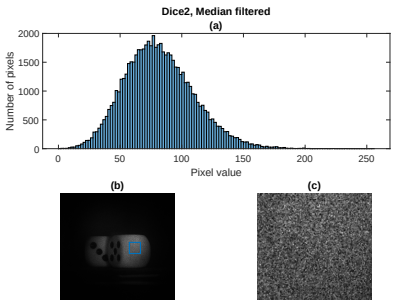

B.4.7 Median

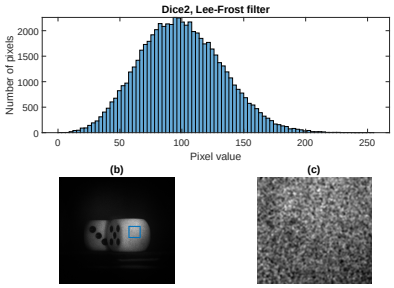

B.4.8 Lee-Frost

Figure B.4: Speckle noise filtering on an optically recorded digital hologram "Dice2", (a) Histogram of the highlighted area, (b) Image, (c) Highlighted area

Chess

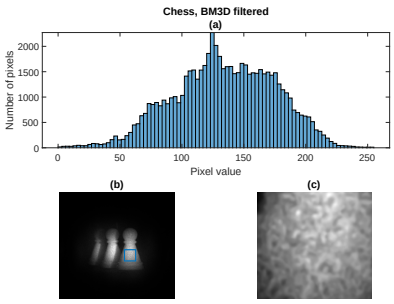

B.5.1 BM3D

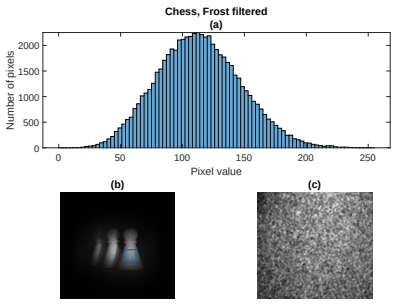

B.5.2 Frost

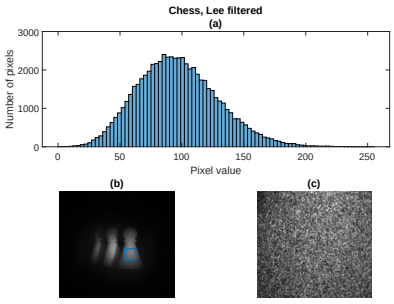

B.5.3 Lee

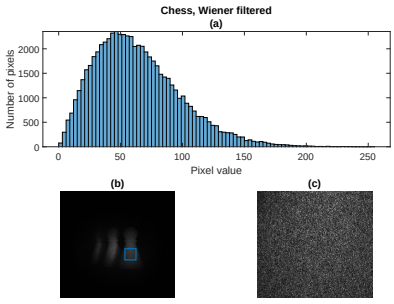

B.5.4 Wiener

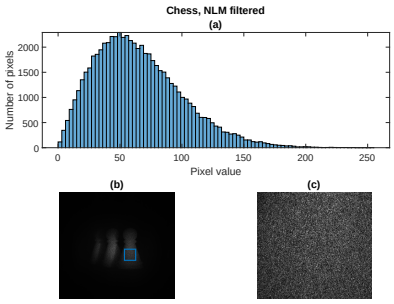

B.5.5 NLM

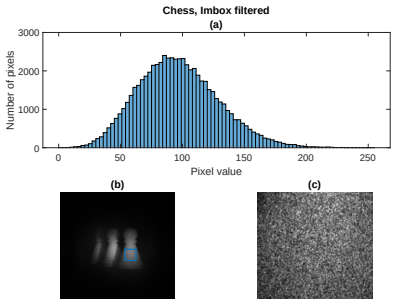

B.5.6 Imbox

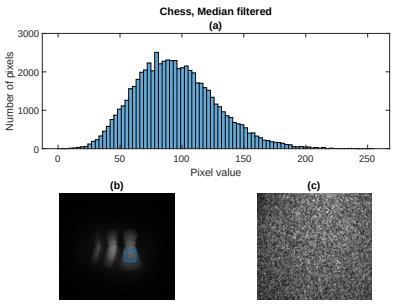

B.5.7 Median

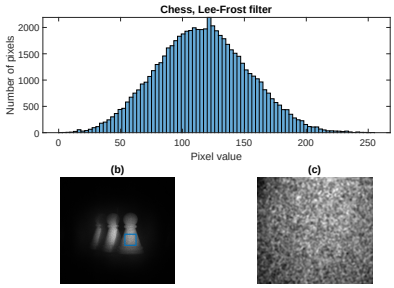

B.5.8 Lee-Frost

Figure B.5: Speckle noise filtering on an optically recorded digital hologram "Chess", (a) Histogram of the highlighted area, (b) Image, (c) Highlighted area

Skull

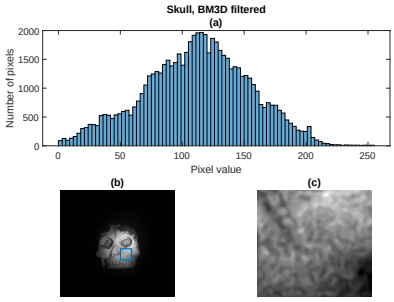

B.6.1 BM3D

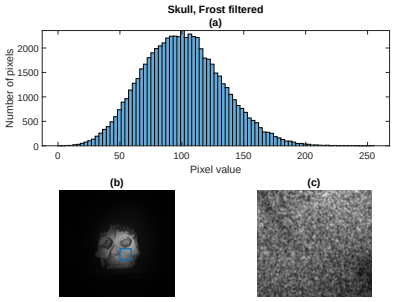

B.6.2 Frost

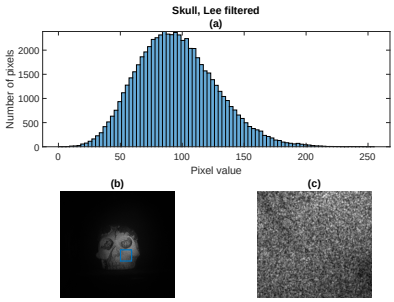

B.6.3 Lee

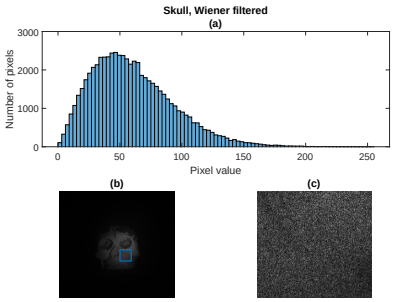

B.6.4 Wiener

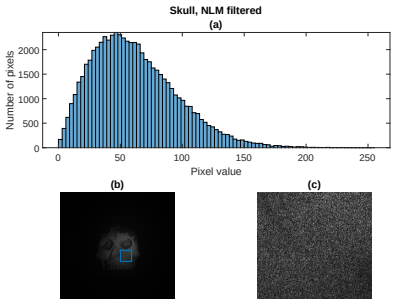

B.6.5 NLM

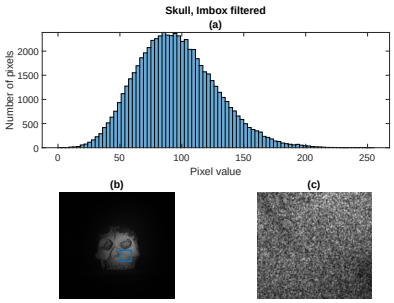

B.6.6 Imbox

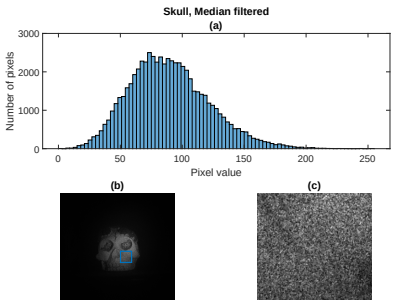

B.6.7 Median

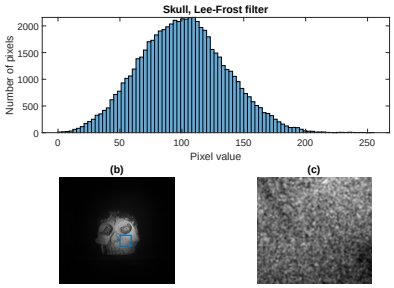

B.6.8 Lee-Frost

Figure B.6: Speckle noise filtering on an optically recorded digital hologram "Skull", (a) Histogram of the highlighted area, (b) Image, (c) Highlighted area

Appendix C

Optically recorded holograms, evaluation

Astronaut

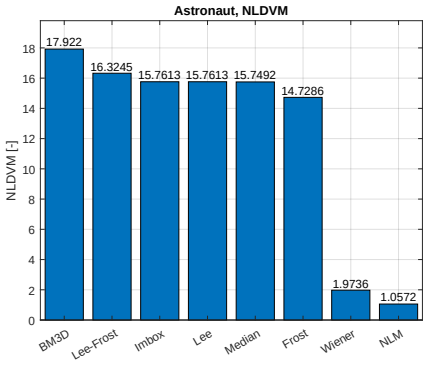

C.1.1 NLDVM

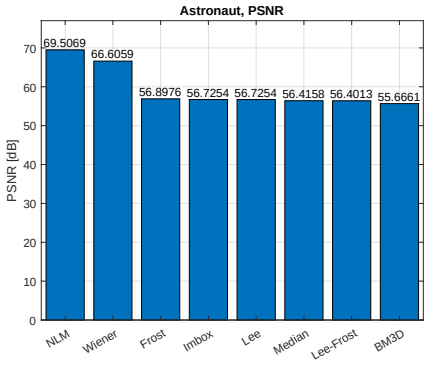

C.1.2 PSNR

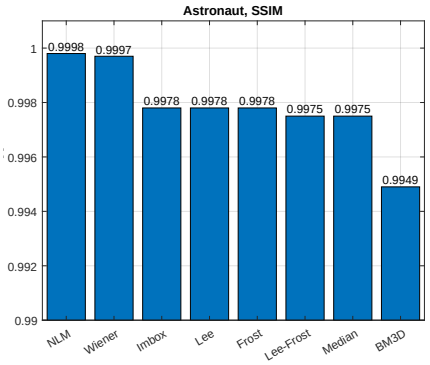

C.1.3 SSIM

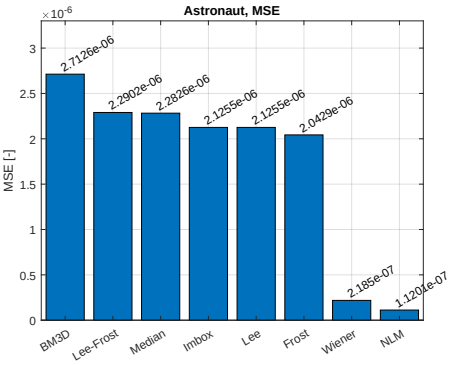

C.1.4 MSE

Figure C.1: Used objective metrics to evaluate the filtration done on the "Astronaut" hologram

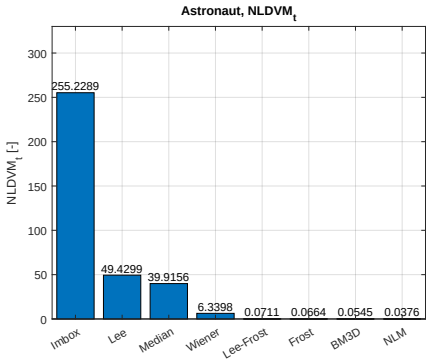

C.2.1 NLDVM$_t$

Computational time, "Astronaut"	
Filter	Time [s]
BM3D	328.68
Frost	221.94
Lee	0.32
Wiener	0.31
Non-Local Mean	28.09
Imbox (2-D Box)	0.07
Median	0.39
Lee-Frost	229.59

C.2.2 Computational time, "Astronaut"

Figure C.2: Effects of the computational time on the NLDVM assessment method, "Astronaut" hologram

Car

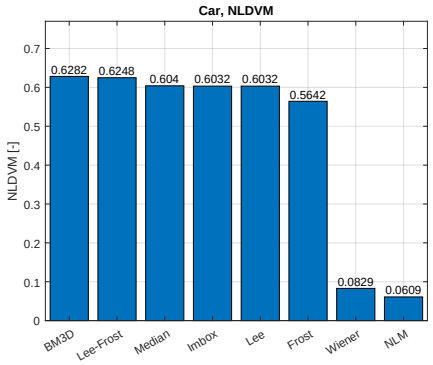

C.3.1 NLDVM

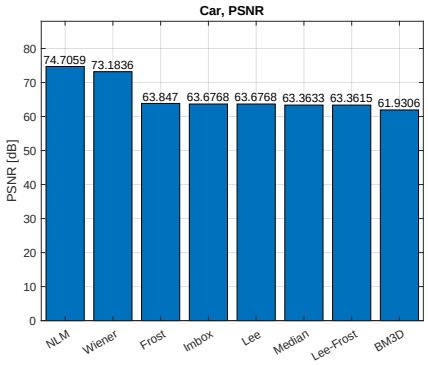

C.3.2 PSNR

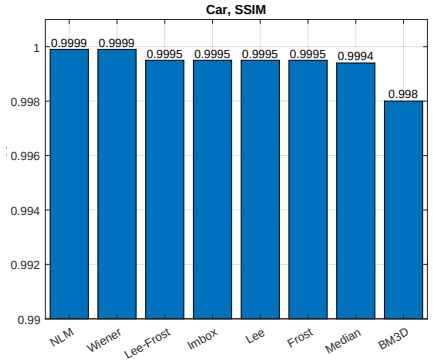

C.3.3 SSIM

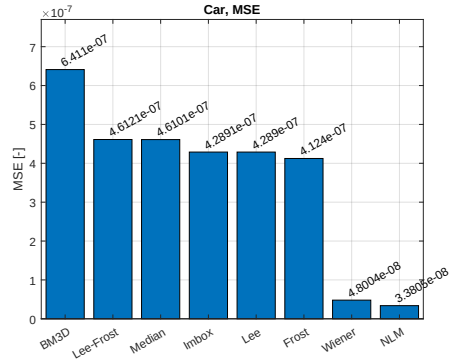

C.3.4 MSE

Figure C.3: Used objective metrics to evaluate the filtration done on the "Car" hologram

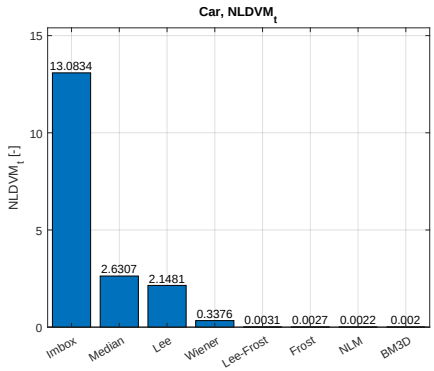

C.4.1 $NLDVM_t$

Computational time, "Car"	
Filter	Time [s]
BM3D	319.08
Frost	205.39
Lee	0.28
Wiener	0.25
Non-Local Mean	27.83
Imbox (2-D Box)	0.05
Median	0.23
Lee-Frost	201.04

C.4.2 Computational time, "Car"

Figure C.4: Effects of the computational time on the NLDVM assessment method, "Car" hologram

Dice1

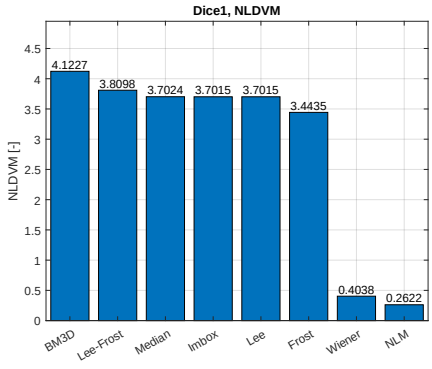

C.5.1 NLDVM

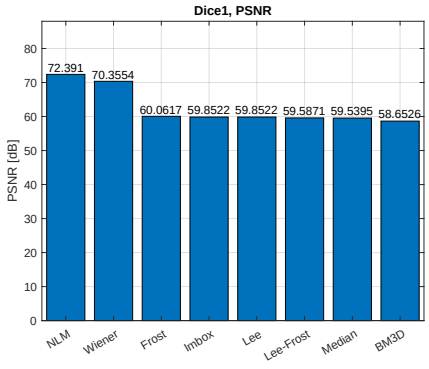

C.5.2 PSNR

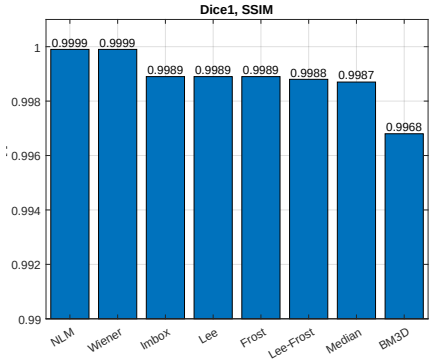

C.5.3 SSIM

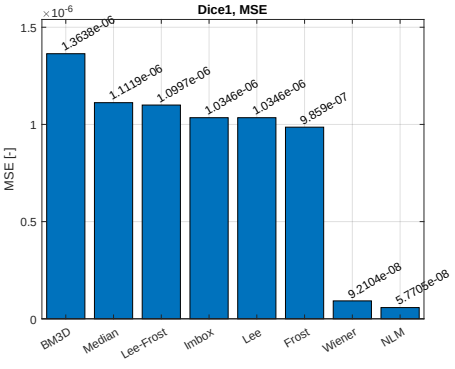

C.5.4 MSE

Figure C.5: Used objective metrics to evaluate the filtration done on the "Dice1" hologram

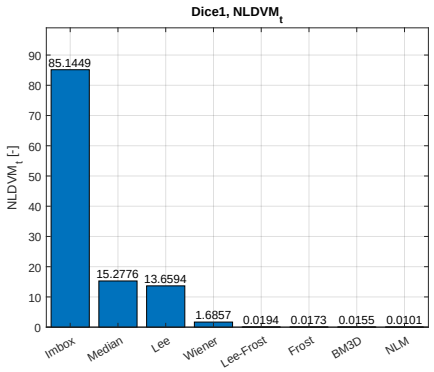

C.6.1 $NLDVM_t$

Computational time, "Dice1"	
Filter	Time [s]
BM3D	266.04
Frost	199.16
Lee	0.27
Wiener	0.24
Non-Local Mean	25.84
Imbox (2-D Box)	0.04
Median	0.24
Lee-Frost	196.89

C.6.2 Computational time, "Dice1"

Figure C.6: Effects of the computational time on the NLDVM assessment method, "Dice1" hologram

Dice2

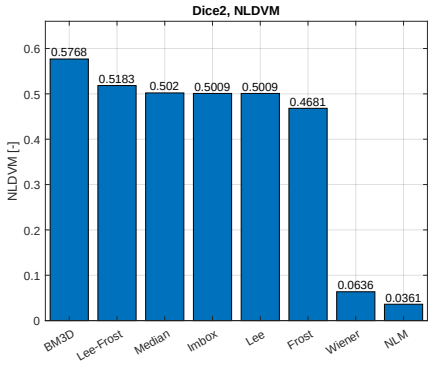

C.7.1 NLDVM

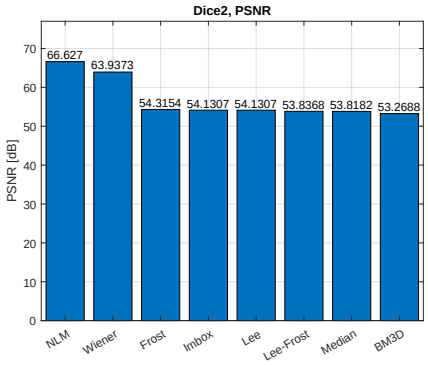

C.7.2 PSNR

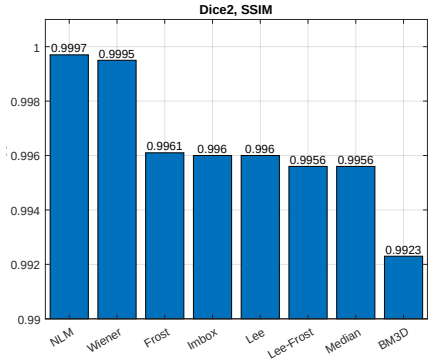

C.7.3 SSIM

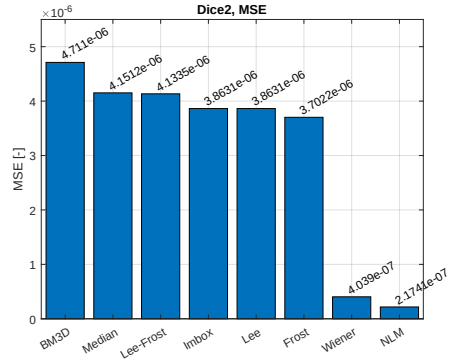

C.7.4 MSE

Figure C.7: Used objective metrics to evaluate the filtration done on the "Dice2" hologram

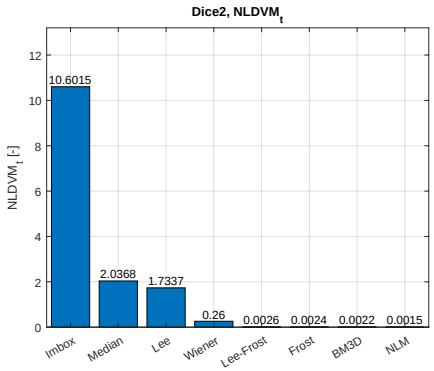

C.8.1 NLDVM$_t$

Computational time, "Dice2"	
Filter	Time [s]
BM3D	267.54
Frost	197.58
Lee	0.29
Wiener	0.24
Non-Local Mean	24.82
Imbox (2-D Box)	0.05
Median	0.25
Lee-Frost	198.87

C.8.2 Computational time, "Dice2"

Figure C.8: Effects of the computational time on the NLDVM assessment method, "Dice2" hologram

Chess

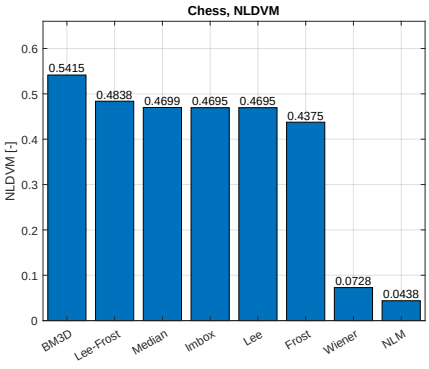

C.9.1 NLDVM

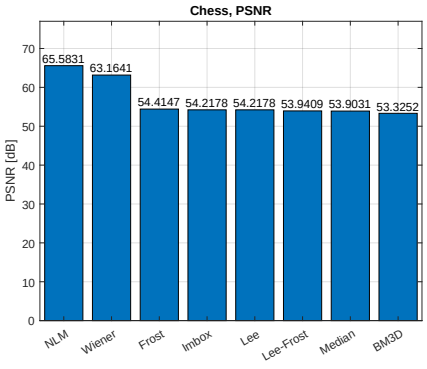

C.9.2 PSNR

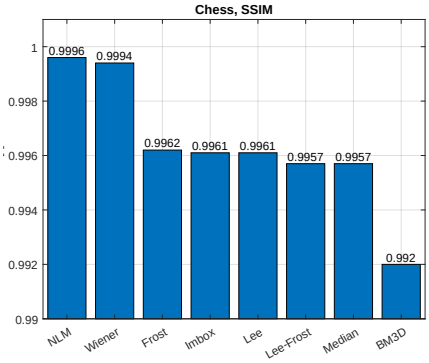

C.9.3 SSIM

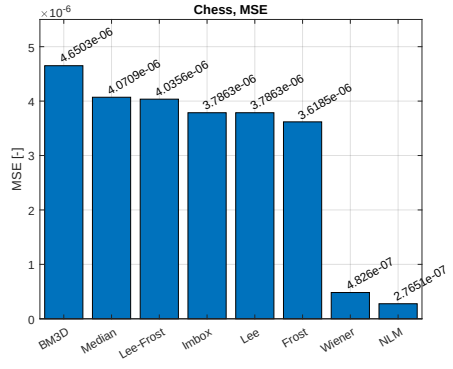

C.9.4 MSE

Figure C.9: Used objective metrics to evaluate the filtration done on the "Chess" hologram

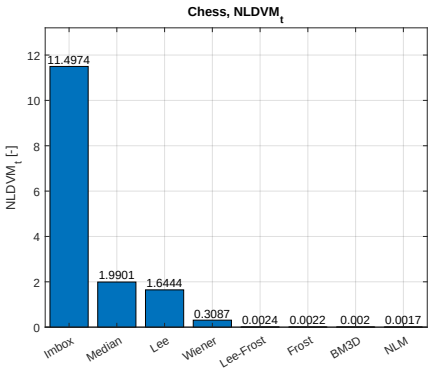

C.10.1 $NLDVM_t$

Computational time, "Chess"	
Filter	Time [s]
BM3D	266.00
Frost	202.83
Lee	0.29
Wiener	0.24
Non-Local Mean	25.94
Imbox (2-D Box)	0.04
Median	0.24
Lee-Frost	201.09

C.10.2 Computational time, "Chess"

Figure C.10: Effects of the computational time on the NLDVM assessment method, "Chess" hologram

Skull

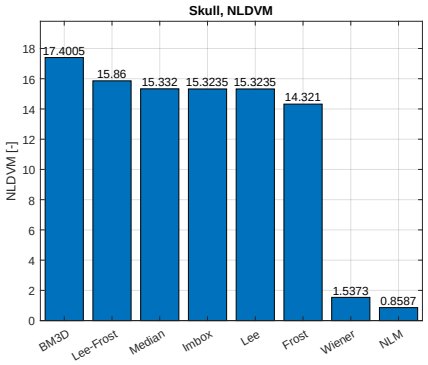

C.11.1 NLDVM

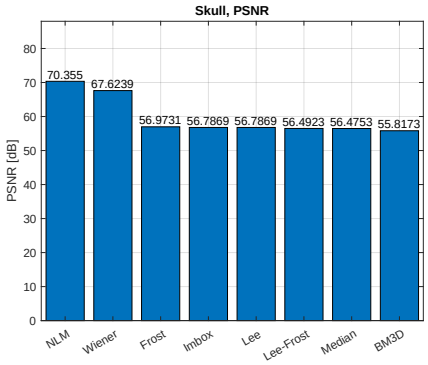

C.11.2 PSNR

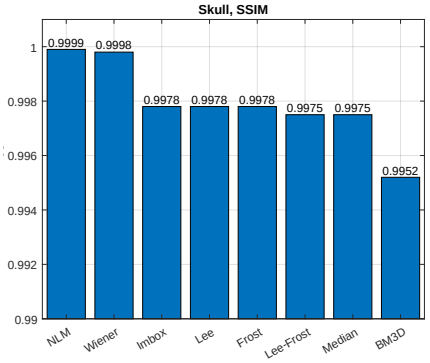

C.11.3 SSIM

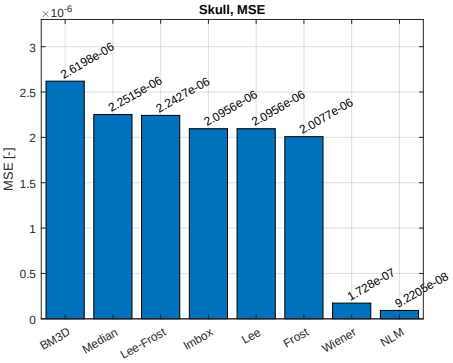

C.11.4 MSE

Figure C.11: Used objective metrics to evaluate the filtration done on the "Skull" hologram

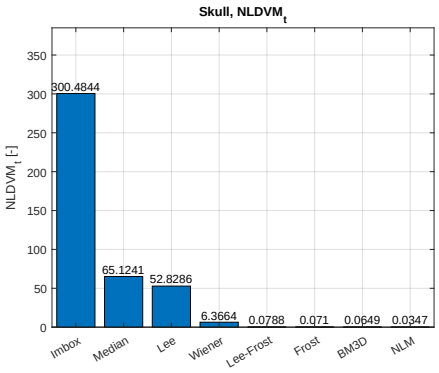

C.12.1 $NLDVM_t$

Computational time, "Skull"	
Filter	Time [s]
BM3D	268.15
Frost	201.65
Lee	0.29
Wiener	0.24
Non-Local Mean	24.74
Imbox (2-D Box)	0.05
Median	0.24
Lee-Frost	201.29

C.12.2 Computational time, "Skull"

Figure C.12: Effects of the computational time on the NLDVM assessment method, "Skull" hologram